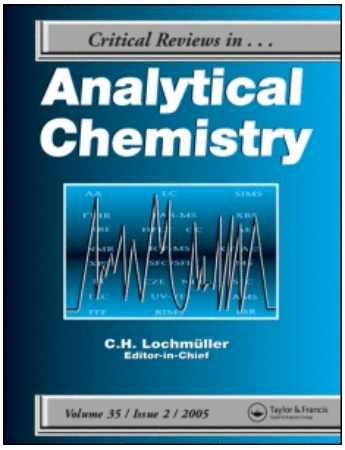

Critical Reviews in Analytical Chemistry
Publication details, including instructions for authors and subscription information:
http://www.informaworld.com/smpp/title~content=t713400837

Graphite Furnaces as Atomizers and Emission Sources in Analytical Atomic Spectrometry

Heinz Falk; Walter Slavin

To cite this Article Falk, Heinz and Slavin, Walter(1988) 'Graphite Furnaces as Atomizers and Emission Sources in Analytical Atomic Spectrometry', Critical Reviews in Analytical Chemistry, 19: 1, 29 — 64
To link to this Article: DOI: 10.1080/10408348808542807
URL: http://dx.doi.org/10.1080/10408348808542807

GRAPHITE FURNACES AS ATOMIZERS AND EMISSION SOURCES IN ANALYTICAL ATOMIC SPECTROMETRY

Author: **Heinz Falk**
Zentral Institut für Optik und Spektroskopie (ZOS)
Academy of Sciences of the German Democratic Republic
Berlin, German Democratic Republic

Referee: Walter Slavin
Department of Advanced Developments
Perkin-Elmer Corporation
Ridgefield, Connecticut; and
Spectrochimistry Acta, B
Pergamon Press, Oxford, England

I. THE ROLE OF ATOMIZERS IN ANALYTICAL ATOMIC SPECTROMETRY

During the last 2 decades, a large variety of procedures for analytical atomic spectroscopy have been developed. This was a result of the need for more and more sensitive and precise methods of trace analysis in various fields of application. Most of the thinkable versions of combinations of the essential parts of the spectrometric arrangements have now been tried out, at least from the theoretical point of view, and often also experimentally. But there are still some possibilities left to form new setups for analytical purposes. This was especially promoted by the advent of tunable lasers as very intense, coherent, and spectrally narrow band radiation sources.[1] Spectroscopic methods originally devoted to fundamental physical or chemical studies have often been exploited as efficient tools for analytical purposes. This fruitful interaction between fundamental and applied research in atomic spectroscopy was recently analyzed by Alkemade.[2]

It is a prerequisite for every procedure in analytical atomic spectroscopy to convert the sample to be analyzed into the atomic form. Samples are mostly in liquid or solid condition and only in some exclusive cases available as free atoms, for example, when mercury has to be determined in the ambient air. Therefore, one can state that atomization is an essential step in any setup for analytical atomic spectroscopy. This step can be followed by a variety of spectroscopic methods such as atomic absorption (AAS), atomic emission (AES), or atomic fluorescence spectrometry (AFS). The first analytical application of atomic spectroscopy by Bunsen and Kirchhoff was based on a flame for both the atomization and excitation of the sample to form the first AES instrument. Other AES arrangements, for example, the electrical arc, the spark, and the inductive coupled plasma (ICP), are characterized by the fact that the conditions for atomization and excitation are inextricably linked because of their working principles. Consequently, it is impossible to optimize these steps independently of each other and the analyst is forced to arrive at a compromise for getting acceptable analytical results. The implications of that coupling between the different steps which are necessary for the atomic spectrometric procedure are underlined, mentioning that the atomization step consists in fact of the substeps of drying, vaporization, and dissociation.

One trend of the recent development in analytical atomic spectrometry can be characterized by the aim to decouple the processes necessary for the analytical procedure for getting well-defined physical conditions for the single process.[3] Such a procedure offers the possibility to minimize the interdependence of the essential analytical steps with the result that unwanted influences, such as matrix effects, can be minimized also or at least they become predictable.

The separate optimization of atomizer systems leads to the concept of coupling an atomizer of this kind with other devices that are very efficient for excitation, for example, a graphite furnace (GF) with an ICP or with a nonthermal plasma of a glow discharge.[3,4] Practical results have shown that this concept can be applied successfully to improve absolute as well as relative detection limits in AES. Of course, the coupling of an atomizer such as a GF to an ICP needs several modifications of the system originally designed for AAS. For such purposes, the range of parameters describing an atomizer has to be defined. This can be done with the help of an adequate model which should be applicable to all atomizers of interest. The various versions of atomizers can be compared with each other and possible reserves for further improvements can be found. In the following, this concept is the guideline that outlines the state of the art in GF technique.

II. DESCRIPTIONS OF ATOMIZERS

A. Types of Atomizers

Starting from the common vaporization techniques applied in AAS, AES, and AFS, such as combustion flame, ICP, or stabilized arc, the most similar electrothermal atomizer (ETA) version is the open electrothermal atomizer.[5] In all these devices a sample vapor is formed that together with the analyte atoms moves freely through the observation volume into the surrounding space. The only peculiarity of an open ETA is the fact that the sample is vaporized from an electrically heated sample support. Then, in all the above-mentioned systems, the analyte atoms pass quickly through the observation volume defined by the dimensions of the measuring beam within the atomic cloud. These systems have in common that analyte atoms leaving the observation volume, e.g., by diffusion, will not be reflected back but get lost by moving into the surrounding space or by condensation on cooler parts of the housing.

If the sample vapor is restricted by the wall of a device heated to the temperature necessary for atomization of the analyte by an electric current flowing through the body of the atomizer, then this device is named enclosed electrothermal atomizer or confined atomizer. The enclosed atomizers have openings where the measuring beam enters and leaves the atomizer and possibly a further opening where the sample may be introduced. Because of the reflection of analyte atoms from the heated wall of the enclosed atomizer and the reduced velocity of the protective gas within the atomizer volume the residence time of the analyte atoms is greatly prolonged compared to open systems. Enclosed ETAs are mostly in the form of tubes made from graphite, in some cases from other electric conducting high-temperature-resistant materials such as tungsten or tantalum.

There are a variety of various forms of open atomizers where the resistive element being the sample support consists of a rod, a filament, a loop, a strip, a wire, a braid, a boat, etc.

Devices where gaseous species are formed from the analytical sample through chemical reactions essentially at room temperatures will not be dealt with in this paper.[6] The gaseous species is then introduced with the help of a carrier gas into a sampling source such as an ICP or an ETA, but the vapor generation is chemically controlled and, therefore, the basic processes are quite different from those going on in ETA.

B. Denotations Used for Atomizers

A schematic cross section of a (confined) atomizer is shown in Figure 1. The heating of the ETA is accomplished by an electric current flowing through the atomizer body. The sample is introduced with the help of a sample injector through the sampling hole.

To prevent the atomizer material from being oxidized at elevated temperatures it is shielded from the atmosphere by a protective gas or purge gas. Usually, an inert gas is used flowing

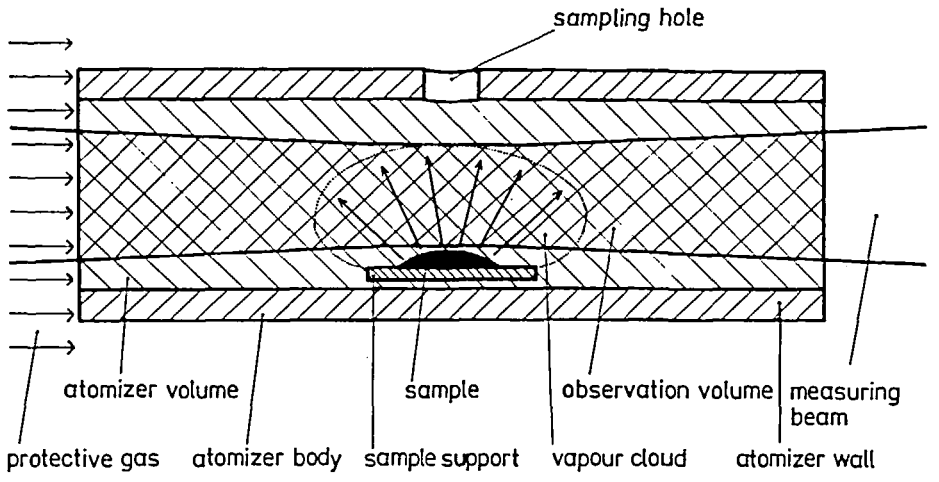

FIGURE 1. Schematic diagram of an atomizer.

around and through the atomizer body forming external and internal gas flows. The latter is responsible for a forced convection inside the atomizer volume.

The sample is placed on the sample support, which may be a part of the atomizer wall (wall evaporation) or may be a separate device inserted into the atomizer body (platform or probe evaporation). The platform or probe is heated mainly by thermal radiation from the hot atomizer body and possibly by electric current. While a platform is permanently present inside the atomizer body, a probe is inserted into a preheated atomizer. The sample, or parts of it, may be transferred by vaporization and condensation from the support to a secondary vaporization surface which is held at a lower temperature.

The sample vapor together with analyte atoms forms a vapor cloud, while the atomizer body is heated to or above the vaporization temperature. The vapor cloud moves freely into the surrounding space under the influence of the protective gas convection in the case of the open atomizer. In confined or semienclosed atomizers, the sample cloud is restricted by the atomizer walls except for the openings where the measuring beam enters or leaves the atomizer. The confined atomizer contains the atomizer volume. A part of this volume defined by the dimensions of the measuring beam is the observation volume. For an open atomizer the observation volume is simply the intersected space between the vapor cloud and the measuring beam.

In the foregoing definitions the term vaporization has been used as the step to bring the sample from the solid into the gaseous phase. In many publications this step is named atomization despite the fact that the sample vapor often leaves the sample support in molecular from. In this case the atomization or dissociation may take place at elevated temperatures within the gas phase of the atomizer volume. In the following, the terms vaporization and dissociation are used where the dissociation may take place at the sample support as well as in the gas phase. In the first case the vaporization of the analyte is at the same time as it is atomized, or the analyte vaporizes in atomic form. The overall process of vaporization and dissociation is named atomization in this paper.

The processes going on in ETAs are governed by their temperature. Analytical samples are treated thermally by a temperature program applied to the atomizer body. There are basically three temperature stages, i.e., drying, pyrolysis or charring, and atomization. A scheme of a temperature program defined by a succession of time intervals with constant (hold) and changing (ramp) temperatures, respectively, is shown in Figure 2. Usually, the atomization stage is followed by the cleaning stage during which the atomizer is heated above the atomization temperature to drive away any residual sample constituents. The

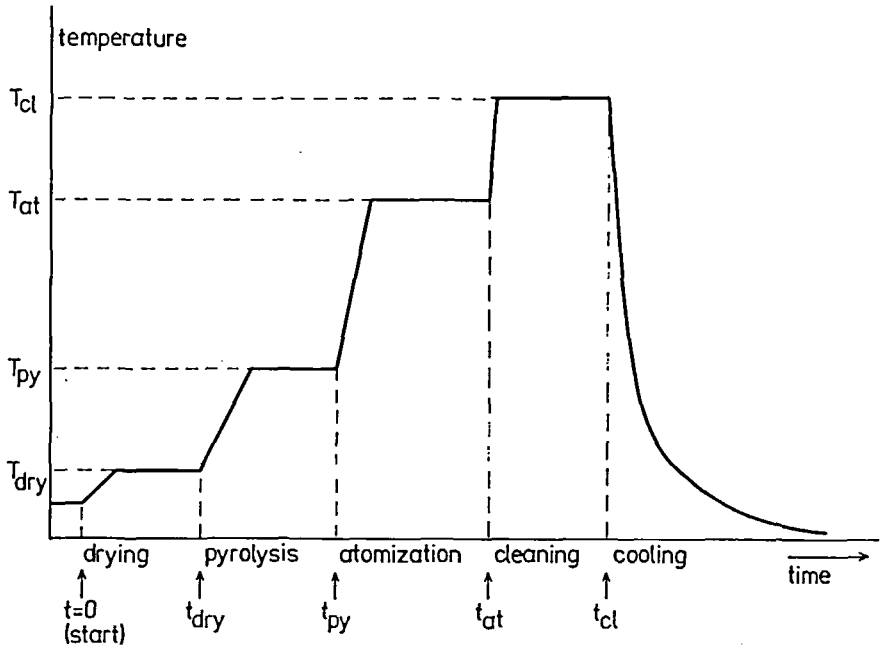

FIGURE 2. Scheme of a temperature program of an electrothermal atomizer.

cooling stage is necessary before the next sample is introduced to allow the atomizer to cool down. This step may also be applied between pyrolysis and atomization stages.

C. Parameters Characterizing Atomization Conditions

The most important parameter of an ETA is its temperature. Depending on the construction of the atomizer there are more or less severe temperature gradients within the system. Therefore, one has to define various temperatures. All these temperatures generally may vary in time and space.

The wall temperature, T_w, describes the temperature of the atomizer body. For a tube atomizer, T_w is a function of the axial coordinate z since the tube ends are in contact with cooled contacts that cause the temperature to drop from the central part to the tube ends. The temperature where the sample is deposited is named surface temperature, T_s. T_s agrees with the platform temperature, T_p, when a platform is used. The temperature of the atomizer volume is described by the gas temperature, T_g, which is generally a function of the time but also of space for a tubular atomizer of the axial and radial coordinates. The heating rate dT/dt in K/s may be defined for all the different temperatures given above, but it usually means the change of the wall temperature in the center of the atomizer body.

A further important parameter of the atomizer is the convection velocity, v_c, of the purge gas within the atomizer volume. The v_c may be determined by a forced flow of the purge gas which applies to the drying and ashing stages where the atomizer volume must be cleared from vapors of the solvent and the matrix, respectively. During the atomization stage, the analyte vapor should be kept as long as possible within the atomizer volume, therefore, the internal gas flow is switched off. This is named the gas stop condition. In this case the remaining velocity of the convective gas flow is determined by the thermal expansion of the purge gas.[7] Of course, the thermal expansion velocity varies strongly with the location in the atomizer volume. The convective flow of the internal purge gas causes an analyte atom loss which rate is determined by the convection velocity. Another loss mechanism always present in an atomizer is the diffusion loss. The rate of atom loss by diffusion is

inversely proportional to the purge gas pressure and will be much increased when an atomizer is operated at low pressures.[3]

As mentioned above, the temperatures characterizing atomizers generally vary in time and space. The time variation of the atomizer during the atomization stage may be drastically reduced if the atomizer temperature is allowed to reach equilibrium conditions before the sample is introduced into the atomizer volume. This mode of operation which can be accomplished by placing the sample on a movable probe or by using separated means for vaporization and atomization of the sample is named constant temperature atomization.[8,9] When the temperature variation of the atomizer body and, therefore, of the gas temperature is reduced during the atomization stage by using a platform, stabilized temperature atomization is said to take place.[10]

Another approach to achieve constant temperature atomization is the second surface atomization. Here, the analyte is collected on a cooled section of the inner surface "the second surface" of the atomizer by condensation. When the atomizer nearly reaches the equilibrium temperature, the second surface is allowed to heat up, releasing the analyte into the hotter environment with nearly constant temperature.[11]

D. Parameters Characterizing the Analyte

Because of the different physical and chemical properties of various sample materials for given atomization conditions the behavior of the analyte will vary. The following parameters describe the situation.

The vaporization temperature, T_{vap} , is the temperature of the sample support at which the analyte begins to enter the vapor phase. The analyte may vaporize in atomic as well as in molecular form. T_{vap} depends on the chemical constitution of the sample, therefore, T_{vap} may be influenced by adding chemical substances called matrix modifiers, which undergo chemical reactions with the analyte.[12] Matrix modifiers usually return the analyte to higher temperatures to permit higher char temperatures which will remove matrix compounds that will otherwise interfere.

The number of analyte atoms evaporated from the sample support per second is called the vaporization rate and is expressed in atoms. Essentially, the vaporization rate is determined by the activation energy of release, E_a, which is a function of both interacting components, the sample support material, and the substance containing the analyte.

The appearance temperature, T_{ap} , is the temperature of the atomizer body at which the analytical signal reaches a certain level. In the case of AAS, this level corresponds to 1% absorptance (0.0044 absorbance) when the quantity of analyte in the atomizer is one thousand times the characteristic mass for peak height absorption. At T_{ap} a certain number of free atoms are present in the observation volume.

If the analyte is evaporated in molecular form, then these molecules have to be dissociated in the gas phase of the atomizer. The degree of dissociation, $\alpha(T_g)$, of the molecules containing the analyte depends on the gas temperature. At a given temperature $\alpha(T)$ is mainly determined by the dissociation energy, E_d, of the molecules.

The actual number of analyte atoms present in the observation volume results from the supply and removal of analyte atoms to and from that volume. The supply is mainly controlled by the temperature program via the activation energy of release and the dissociation energy. The removal depends on the losses by diffusion and convection.

E. Atomizer Efficiency

It is the purpose of an atomizer to transform a liquid or solid sample into an atomic vapor and to keep that vapor within the observation volume during the measuring time. Furthermore, it is advantageous for the analytical performance of the atomizer if the analyte atoms and the matrix vapor will appear at different times in the observation volume.

The action of the atomizer may be described by the atomic density of the analyte within the observation volume which generally depends on time and space:

$$n_a(t, x, y, z) = \epsilon_a(t, x, y, z) * \dot{N}_s(t) \quad (1)$$

The time-dependent sampling rate $\dot{N}_s(t)$ introduced into the atomizer gives rise to the atomic density $n_a(t,x,y,z)$ via the characteristic transfer function $\epsilon_a(t,x,y,z)$ where t,x,y,z are the time and space coordinates, respectively. The symbol "*" stands for a convolution which, in the simplest case, is a multiplication.

For atomizers with continuous sample introduction such as flames, ICPs, or stabilized arcs using constant flow nebulization devices, steady-state conditions will be reached and the time dependence of the atomic density vanishes during the measurement. For a selected observation volume the density anisotropy is negligible and the atomic density becomes

$$n_a = \dot{N}_s \eta_t \tau_r \alpha(T)/V_a \quad (2)$$

Where $\dot{N}_s$ is the sample aspiration rate, η_t is the fraction transported into the atomizer volume, $\alpha(T)$ is the degree of dissociation of the analyte at the temperature T, and V_a is the observation volume. In an "ideal" atomizer, all analyte atoms introduced during a suitable measuring time, Δt, would be present in atomic form within the atomizer volume and, consequently, the atomic density will be

$$n_{ai} = \dot{N}_s \Delta t/V_a \quad (3)$$

Using this, the "atomizer efficiency" for continuous sample introduction will be

$$\eta_a = \frac{n_a}{n_{ai}} = \eta_t \tau_r \alpha(T)/\Delta t \quad (4)$$

When applying Equation 4, it should be noticed that the sample consumption per measurement is determined by the measuring time Δt plus the time necessary for the atomizer to reach steady-state conditions.

In pulsed atomizers such as GFs or "flow injection" systems[13] the atomic density becomes time dependent:

$$n_a(t) = f_{sl}(t, \tau_e, \tau_r)N_s \eta_t \alpha(T)/V_a \quad (5)$$

where $f_{sl}(t, \tau_e, \tau_r)$ is the supply-loss-function, τ_e and τ_r are the evaporation and residence times, respectively, N_s is the given number of analyte atoms of the sample. Under ideal conditions the evaporation time is much shorter than the residence time and the residence time is larger than the measuring time. Then f_{sl} is a rectangular function with the amplitude unity and duration Δt and the atomic density within the ideal atomizer becomes

$$n_{ai} = N_s/V_a \quad (6)$$

With regard to the maximum density during the transient signal the atomizer efficiency in this momemt may be defined:[14]

$$\eta_{ap} \equiv \frac{n_{ap}}{n_{aip}} = f_{sl}(t_p, \tau_e, \tau_r) \eta_t \alpha(T) \quad (7)$$

In fact, any measurement needs a finite time interval t_1 to t_2 wherein the time average of the atomic density within the observation volume is observed:

$$\bar{\eta}_a(t_1, t_2) \equiv \int_{t_1}^{t_2} n_a(t)\, dt/(t_2 - t_1) \tag{8}$$

On this basis the general definition of the atomizer efficiency becomes

$$\eta_a \equiv \frac{\bar{n}_a}{n_{ai}} = V_a \int_{t_1}^{t_2} n_a(t)\, dt/(N_s\, \Delta\, t) \tag{9}$$

with $\Delta t = t_2 - t_1$.

III. TECHNICAL AND PHYSICAL FEATURES OF ELECTROTHERMAL ATOMIZERS

A. Applicative Aspects

By far, most of the applications of electrothermal atomizers have been for AAS.[15] Therefore, the technical perfection of enclosed electrothermal atomizers, which are most suited for AAS, is very high. These systems are essentially described in Figure 1. The dimensions of the tube furnace range from 3 to 8 mm in diameter and 15 to 40 mm in length. The actual size of tube furnaces depends on the sample amount to be analyzed. Roughly, the atomizer volume has to be ten times larger than the sample amount converted to a vapor at analytical temperature. The reason for the preference of the tube configuration in AAS applications is the optimum compromise between relatively long residence times for the analyte vapor and a sufficiently high optical throughput to carry out absorption measurements. Additionally, the intense thermal light emission may be suppressed very efficiently.

When electrothermal atomizers are used in atomic emission work, the demands to be fulfilled are very similar to those known from AAS. The observation angle for the emitting volume has to be large, but scattered light from the hot atomizer wall must be avoided. For AES purposes also, the tube furnace is the optimum configuration.[3,16]

Electrothermal atomizers to be used for atomic fluorescence spectrometry have to allow both very intense illumination with the excitation wavelength and, from a different direction, the measurement of the fluorescence signal with as high as possible optical conductance.[1] Stray light from incandescent parts of the atomizer is very critical in LAFS. Under these circumstances, an open system such as a heated cup appears to be a reasonable approach.[17] Of course, the cup atomizer needs a permanent flow of purge gas or even evacuation to be prevented from oxidation.[17] Consequently, the atomizer efficiency is lower than in a confined atomizer but this can be compensated for by the higher absolute detection capability of laser-excited AFS compared to AAS.[18]

Besides the atom formation from a sample, electrothermal atomizers may also be applied as vaporizers in connection with emission sources.[19,20] Similar to other nebulizers, the atomizer forms an aerosol of the sample material to be transported into the excitation source such as an ICP. These "electrothermal vaporizers" allow a better desolving of the sample aerosol compared to pneumatic or ultrasonic nebulizers. Because of the carrier gas flow necessary to transport the sample aerosol, electrothermal vaporizers consist essentially of a cup or rod configuation. Vaporizer systems are not be considered further in this paper.

B. Basic Constructive Designs of GFs

Constructive details of the large variety of GFs described in the literature are not given.

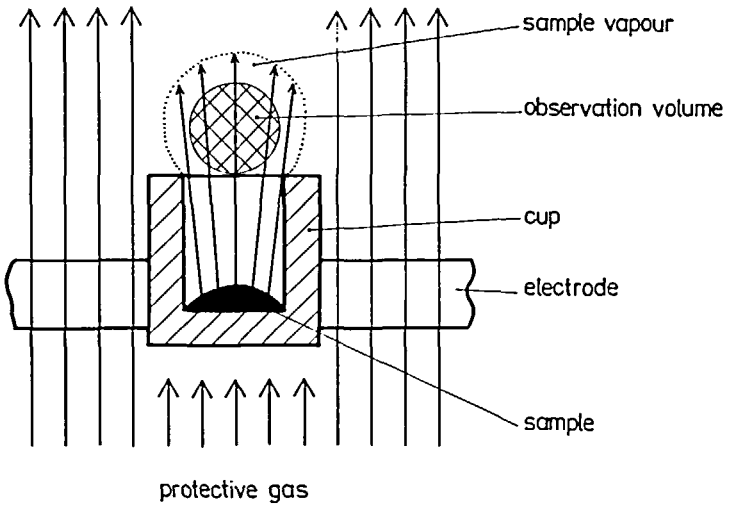

FIGURE 3. Schematic view of a cup-type atomizer. Contact ports and housing are omitted.

Such information, including comparative considerations, may be found in several other publications.[15,21,22] There are three basic configurations: open cup or rod systems, pulse-heated tube furnaces, and constant-temperature furnaces which are shown in Figures 3 to 5.

Open atomizers have in common that the purge gas flow has to be maintained when the cup is heated. Consequently, there is a forced gas flow during the atomization stage that dilutes the atomic cloud above the cup. Thermal expansion cannot be avoided during the heating stages of electrothermal atomizers, but open systems are additionally influenced by thermal convection of the purge gas.

Enclosed atomizers are usually equipped with the means to maintain an inner purge gas flow during drying and charring stages to allow the released vapors to be cleared from the furnace. For the atomization stage, the inner gas flow can be stopped with the result that analyte losses will be greatly reduced. Pulse-heated furnaces that are able to carry out all the steps from drying to atomization are relatively simple to operate. Movable parts are only necessary for the sampling device. One power supply is sufficient to heat this so-called "Massmann furnace".[23] The ease of operation of the Massmann design is connected to the drawback that volatilization of the sample and furnace temperature cannot be controlled separately. From that fact the need arises to bring the furnace rapidly to the required final temperature, a point which will be dealt with later in this paper. Capacitive heating followed by resistive heating to maintain the temperature offers a possibility to get very high heating rates. This operation mode has been suggested by L-vov[24] and was later used extensively by Chakrabarti and Chang.[25]

The original GF design of L'vov used a constant temperature atomizer. In this arrangement the sample was volatilized from an independently heated electrode after the heated tube was no longer changing in temperature. The same principle has been applied in a more recent version developed by Frech et al., consisting of a graphite cup fitted tightly into an aperture in the bottom of a graphite tube.[9] One pair of graphite rods contacted the cup and another pair of rods contacted the tube (see Figure 5). Independent power supplies raised the cup and tube to (nearly) independent temperatures, thus permitting the heating of the tube until it was at a nearly constant temperature before vaporizing the sample. Means for a purge gas around and through the tube are provided. Other versions of constant temperature furnaces

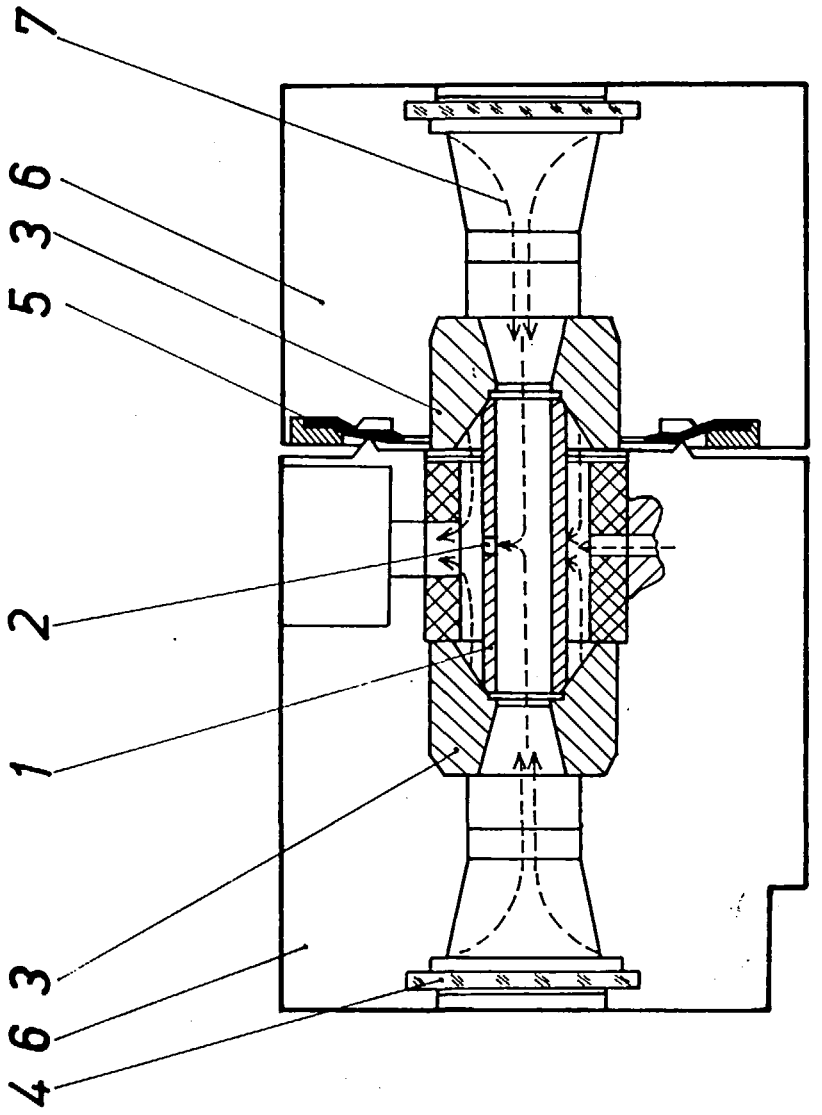

FIGURE 4. Cross-sectional view of a tube atomizer for AAS. 1, Graphite tube; 2, sampling hole; 3, contact electrodes; 4, window, 5, lip seal; 6, housing (water cooling omitted); 7, purge gas.

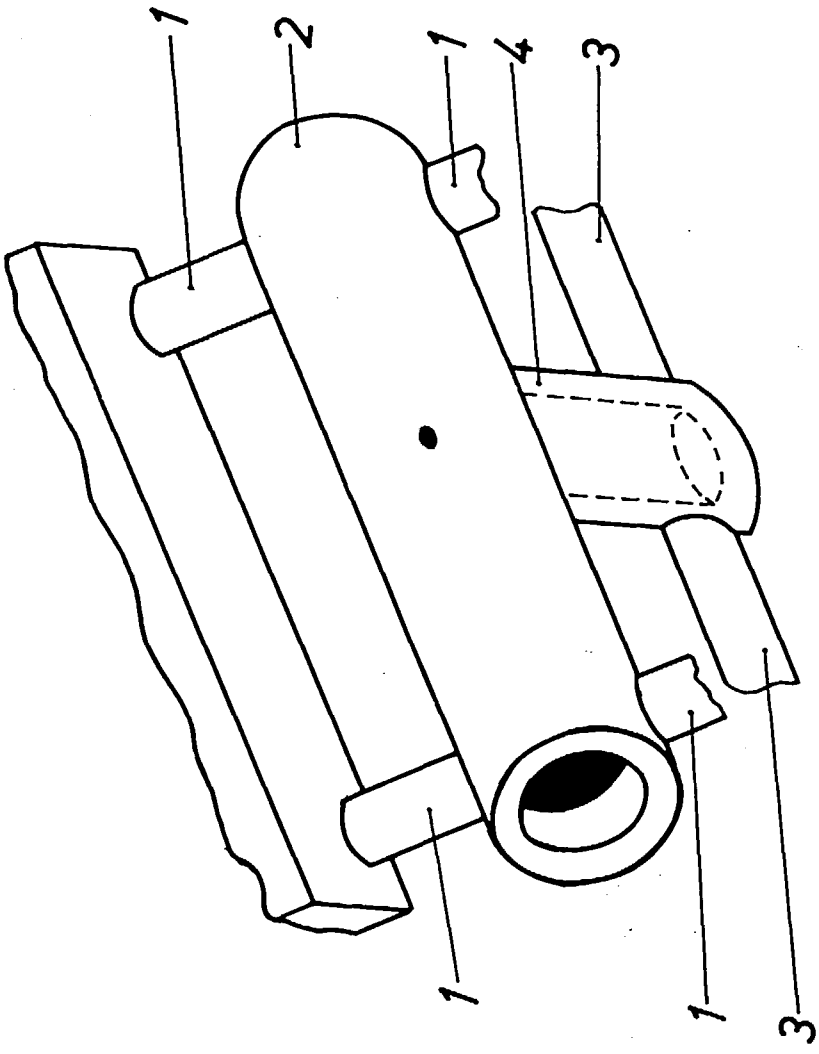

FIGURE 5. Schematic view of a constant temperature (two supply) furnace for AAS. 1, Electrodes for the graphite tube; 2 and 3, electrodes for the graphite cup (4).

have been studied by Woodriff et al.[22] Atomizers of that kind are more complex in construction and operation but they allow the ultimate analytical performance, since the temperatures for volatilization and atomization can be optimized.

A relatively simple way of achieving nearly constant temperature atomization consists in the deposition of the sample on a separate sample support inside the tube, a platform or a probe (see Section II.B). In particular, the platform is relatively easy to install but its temperature is not independent of that of the tube. There is only a limited temperature difference achievable between tube and platform temperatures.[27]

C. Temperature Characteristics of GFs

Whereas temperature gradients above a cup of an open atomizer cannot be avoided, the lengthwise temperature distribution of a tube atomizer is expected to be much more uniform. Of course, at the tube ends, because of heat tansfer to the cooled electrodes, the tube temperature must drop. The question is what part of the tube length may be considered as being at constant temperature or at what distance from the center do analyte losses occur because of molecule formation and condensation.

Let us first discuss the equilibrium case, i.e., the temperature distribution of the tube under stationary conditions. Then, the temperature of the tube wall is a function of the axial coordinate z only, e.g., a Gaussian distribution:[28]

$$T_w(z') = T_0 \exp(-\gamma z')^2 \quad (10)$$

where T_o is the temperature at the center, γ is the parameter describing the deviation from isothermal conditions, $z' = z/l$, l is the tube length. Equation 10 is valid for tubes with constant cross-section of the wall. Their lengthwise gradient is as much as 1000 K when the tube is at 2800 K at the center.

This gradient can be greatly reduced by using contoured tubes in which the wall thickness is decreased at the ends as proposed by Slavin et al.[29] Using a suitable function of the wall thickness with the tube length, an extended region of constant tube temperature can be achieved. Examples for such lengthwise temperature distributions, $T_w(z)$, are shown in Figure 6. As can be seen from this figure, the shape of $T_w(z)$ varies with the temperature at the center. This behavior results from the fact that at temperatures below 1500 K the heat loss by conduction is dominating, whereas at higher temperatures thermal radiation losses increase. The equilibrium temperature distribution of a graphite tube is of a practical interest for constant temperature atomizers such as shown in Figure 5.

When a Massmann furnace is used where rapid temperature changes take place during the atomization stage, the dynamic distribution has to be considered. Measurements of the time-dependent temperature distribution of graphite-tube atomizers have been carried out by Falk et al.[30] Some of their results are shown in Figures 7 and 8. From these experimental results, it can be seen that the axial temperature distributions during the ramp stage are quite different from those after reaching equilibrium. At high ramp rates starting at ambient temperature, the tube temperature is practically constant in the central part with a length of 20 mm. In the equilibrium situation there is a temperature gradient of 600 K over this length. As shown in Figure 8 there is already a small axial gradient in the central part of the tube during the ramp stage at a ramp rate of 1000 K/s.

The results of the dynamic measurements of axial tube temperatures can be summarized as follows. The initial temperature gradient for more than two thirds of the tube length is conserved when a fast heating rate (>1000 K/s) is applied; especially starting from room temperature with fast heating results in a flat distribution around the center during the ramp stage. About 1 sec after ending the ramp stage this deviation from equilibrium has vanished.

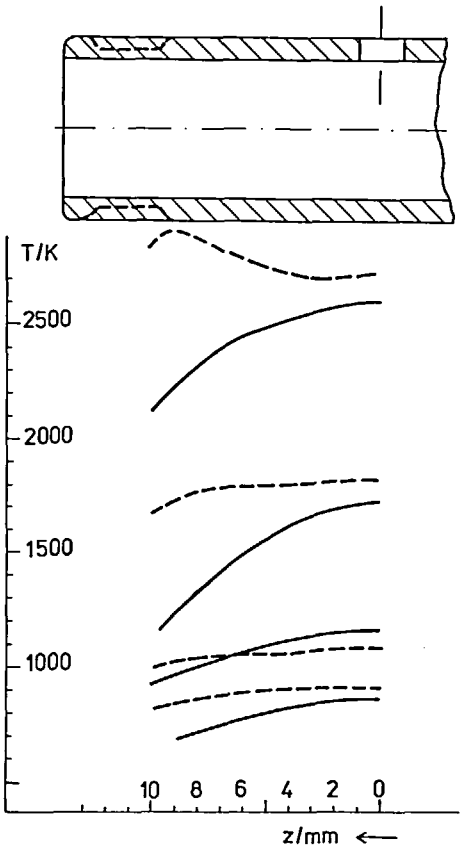

FIGURE 6. Lengthwise temperature distributions of usual and contored graphite tubes for different temperatures.

This finding can be understood by discussing the expression for the heating rate

$$d\,T_w/dt = (P_a - P_\ell)/C_{st} \quad (11)$$

where P_a is the applied electric power, P_ℓ is the overall heat loss, and C_{st} is the heat capacity of the tube. Since P_ℓ is a function of the temperature and the distance from the center, the heating rate becomes constant if $P_a \gg P_\ell$ is valid. This condition can be met for most of the tube length where the conduction losses to the end contacts are not very high.

The flat axial temperature distribution of the tube atomizer at high heating rates starting at low temperatures has some practical consequences. Under these circumstances the length of the isothermal zone of the tube is extended considerably. Consequently, these conditions are optimum for analytical purposes, which is also suggested by the finding that a "cool-down step" before atomization is advantageous.[31]

Contoured tubes that are more massive in the central part than near the ends experience a higher heating rate at the thinner parts. Therefore, the possible ramp rate is limited by the fact that an overheating near the ends must be avoided. Therefore, the heating rate at the center where the sample is deposited will be decreased.[29,32] The result is a lower atomic density, in particular for refractory elements. In conclusion, it can be stated that contoured tubes are not suited to improve the efficiency of Massmann type furnaces considerably. In connection with platforms, contoured tubes in several cases show a slightly higher tolerance against matrix influences.[32] This can be explained by the shift of the sample evaporation into the isothermal region.

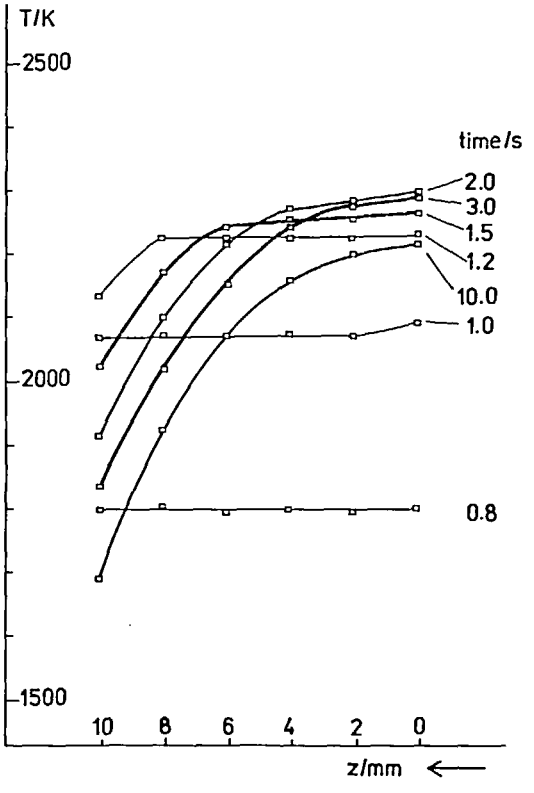

FIGURE 7. Axial temperature distribution of a graphite tube with pyrolytic coating.[30] Tube length — 28 mm, internal diameter — 6 mm, external diameter — 8 mm, linear ramp rate at the center — 1.8 kK/s starting at ambient temperature.

D. Temperature Characteristics of Platforms

Typical platform geometries are given in Figures 9 thru 11.[27] The platforms shown in Figures 9 and 10 have in common that they bridge a part of the voltage drop along the length of the tube when the tube is heated by an electric current. Therefore, besides thermal radiation and heat conduction from the hotter tube wall, the electric current passing through the tube contributes directly to the heating of these platforms. In contrast, the pin platform shown in Figure 11 is subject to heating by radiation and heat conduction only. As a consequence, the time lag between the heating of the tube and the platform is expected to be greater for the pin platform. This was experimentally verified by Falk and Glismann.[27] Figures 12 and 13 show examples of the calculated temperature differences between the wall and platform during the atomization stage. The parameters of the theoretical model upon which the calculations were based have been evaluated from pyrometric temperature measurements of tube wall and platforms.[27]

The maximum temperature difference between the tube and platform appears at the end of the ramp stage of the tube. The amount of this difference ranges from 300 to 600 K in the temperature interval 1000 to 2000 K and it increases when the ramp starts at lower temperature and vice versa.

Roughly, the said temperature difference can be approximated by a triangular function where the leading edge is steeper than the falling edge. Also under equilibrium conditions, the temperature of the platform remains lower than that of the wall. This effect increases at higher temperatures up to 300 K, depending on the configuration which explains the special difficulties of evaporating samples with high boiling points from platforms.

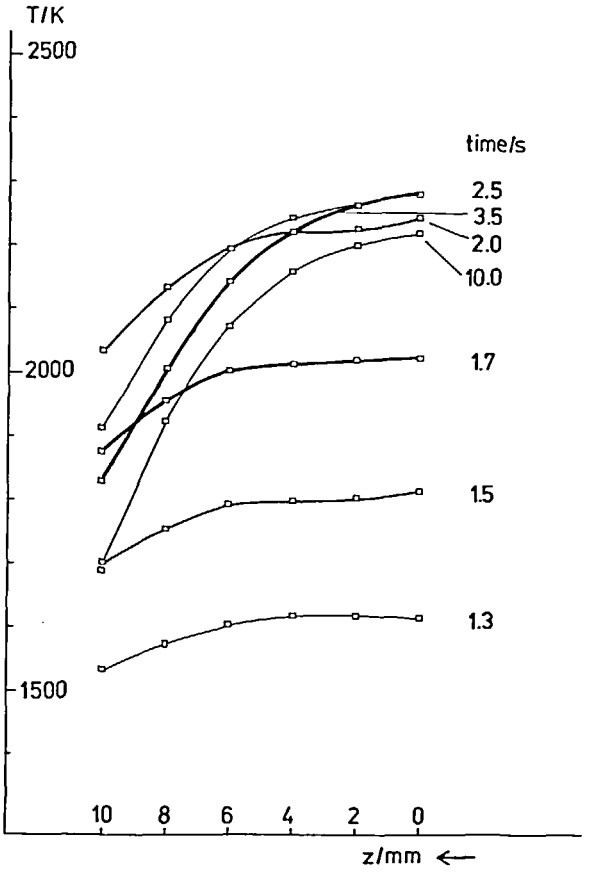

FIGURE 8. Axial temperature distribution of a graphite tube with pyrolytic coating.[30] Tube length — 28 mm, internal diameter — 6 mm, external diameter — 8 mm, linear ramp rate at the center — 1 kK/s starting at ambient temperature.

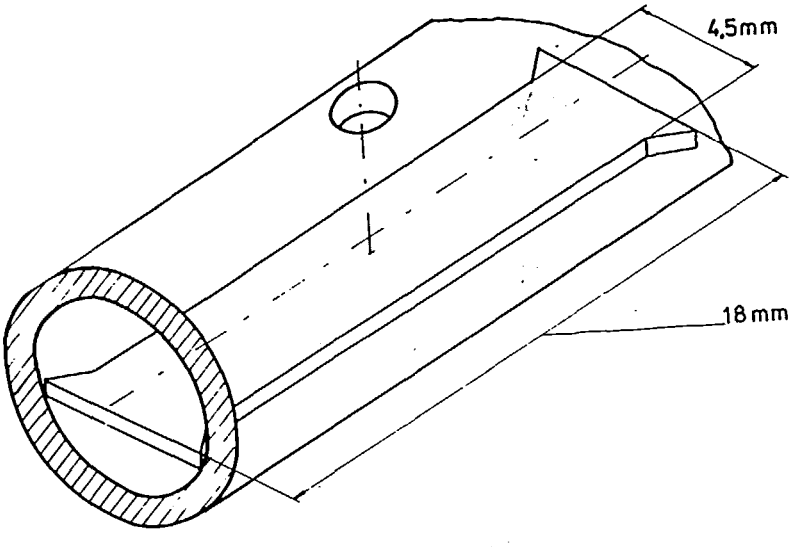

FIGURE 9. Geometry of the L'vov platform. l_a = 28 mm, d_a = 6 mm.

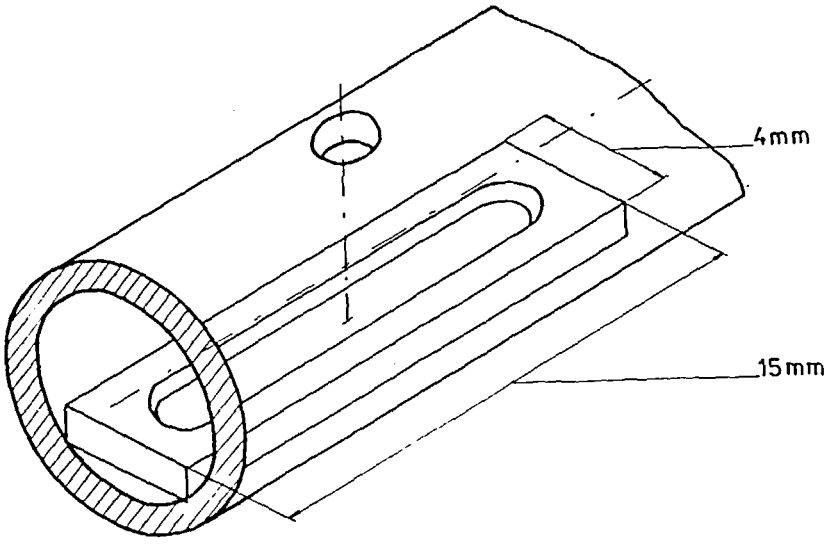

FIGURE 10. Geometry of the Perkin-Elmer platform. l_a = 28 mm, d_a = 6 mm.

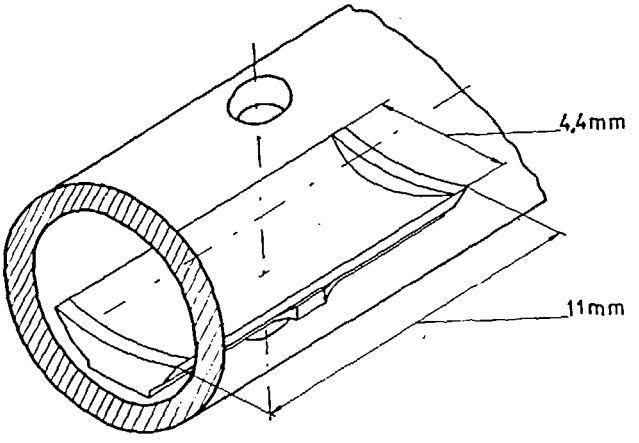

FIGURE 11. Geometry of the pin platform.[27] l_a = 28 mm, d_a = 6 mm.

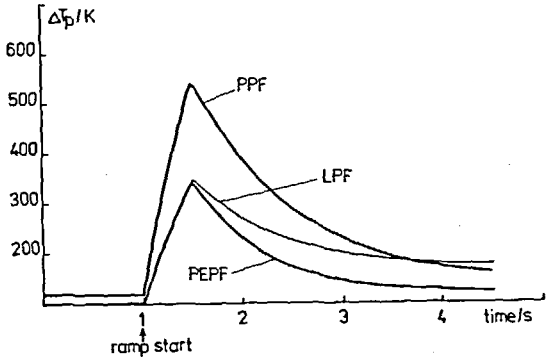

FIGURE 12. Difference between platform and tube temperatures.[27] The tube temperature is increased from 1270 to 2270 K with a ramp rate of 2 kK/s starting at 1 s. PPF-pin platform, LPF-L'vov platform, PEPF-Perkin-Elmer platform.

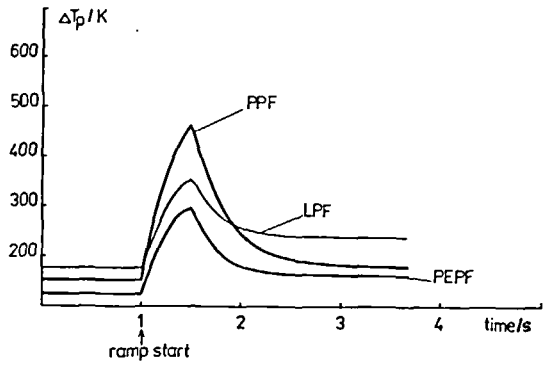

FIGURE 13. Difference between platform and tube temperatures.[27] The tube temperature is increased from 2270 to 3270 K with a ramp rate of 2 kK/s starting at 1 s. PPF-pin platform, LPF-L'vov platform, PEPF-Perkin-Elmer platform.

IV. MODEL CALCULATIONS OF THE ATOMIC DENSITY IN GFs

A. Formulation of the Model

There are a number of publications dealing with the description of the processes going on in GFs that will enable one to find an adequate description of the system under the influence of the numerous parameters affecting it. The most recent contribution to this topic has been given by Chang and Chakrabarti.[25] In the following, the existing model calculations will be expanded to include all relevant influences on the atomic density on the one hand and to apply the model to the pulse-heated furnace with and without a platform and on the other hand, to the constant temperature furnace.

For the sake of simplicity the model starts from the following assumptions.

1. The sample is dispersed on an extremely small area at the middle of the graphite tube.
2. Redeposition of the analyte is neglected.
3. The distribution of the analyte vapor in the gas phase over each transverse cross-sectional plane is uniform.
4. The loss of analyte atoms from the atomizer volume is controlled by diffusion and gas expansion. The analyte atom density falls linearly from a maximum at the middle of the tube to zero at the ends.
5. There is no temperature gradient along the length of the tube and no temperature difference between tube surface and gas phase.
6. The effective path length is essentially equal to the geometric length of the tube.
7. The pressure of the inert purge gas is held constant while operating the furnace.

The assumptions 1 thru 7 represent no severe limitation of the application range of the model. Redeposition effects have been observed in GFs but they are only relevant when the anisotropy of the vapor distribution in the gas phase is of interest.[33] In most experiments the atomic density is averaged over the transverse cross-sectional plane by the measuring system. Assumption 5 is acceptable using the results shown in Section III.C and the fact that temperature differences between the wall and gas phase are small as long as the heating rate is lower than 5 kK/s.[7]

The rate of formation of analyte atoms in the atomizer volume is determined by the rate of volatilization from the surface

$$dX_t/dt = f_s(t, X_t) \quad (12)$$

Table 1
VARIATION RANGES FOR THE DESORPTION CONSTANTS[36]

Constant	Unit	Range
Frequency factor		
A	s^{-1}	10^4—10^{15}
Order of release		
m		0—1
Activation energy		
E_a	$kJmol^{-1}$	30—500
Monolayer coverage		
σ_{mono}	m^{-2}	$\approx 10^{19}$
(σ_{mono}) (M = 50)	$\mu g cm^{-2}$	($\approx$ 0.1)

where X_t is the total number of the preatomization species and $f_s(t,X_t)$, the supply function depending on the time t, via the changing temperature T(t) and on $X_t(t)$. The time variation of the analyte vapor in the gas phase of the atomizer is

$$dY_t/dt = dX_t/dt - f_\ell(t, Y_t) \quad (13)$$

where Y_t is the total number of analyte atoms in the gas phase of the atomizer and $f_l(t,Y_t)$ is the loss function. If the analyte evaporates in atomic form, then Y_t is identical with the number of atoms within the observation volume Y_a. For analyte species that are vaporized in molecular form, a subsequent dissociation must take place to form observable analyte atoms.

B. The Release Mechanism

Generally, the release rate of particles adsorbed on a solid surface is given by:[33,34]

$$d\sigma/dt = \Sigma^m A \exp(-E_a/kT) \quad (14)$$

where σ is the surface coverage in units of particles (atoms) m^{-2}, m is the order of release, A is the vibration frequency of the particles perpendicular to the surface, and E_a is the activation energy.

If there is a massive coverage of the surface (bulk material), the release rate becomes independent of the amount of adsorbed material, or m = 0. For coverages in the monolayer and submonolayer range the situation is more complicated.[33] For submonolayers, if the particles interact mainly with the substrate, a first-order release process takes place, i.e., m = 1. Many metals form microdroplets or microcrystallites on the surface. Corresponding to the measurements of Arthur and Cho,[35] it appears to be typical for situations where adsorbate-adsorbate interactions are comparable to adsorbate-substrate interactions, i.e., m = 1/2. Theoretical calculations with the assumption that the interaction between microdroplets takes place only at their borders lead to m = 1/2, which was confirmed experimentally for Cu and Au on a graphite surface.[35] The variation ranges for the constants in Equation 14 are given in Table 1. For further calculations, Equation 14 can be written as follows

$$dX_t/dt = X_t^m A \exp(-E_a/kT) \quad (15)$$

C. The Loss Mechanism

For the loss of analyte vapor by diffusion we have

$$f_{ld} = k_d Y_t(t) \tag{16}$$

where

$$k_d = 8D/l_a^2 \tag{17}$$

D is the diffusion coefficient and l_a is the tube length.[37] The temperature dependence of the diffusion coefficient may be expressed as follows

$$D = D_0(T/T_0)^n \tag{18}$$

where D_o is the diffusion coefficient at stp (T_O = 273 K), and the value of n (to be called gas combination factor) varies from 1.5 to 2.0 for various combinations of gases.[37] For D_o one has the following expression:[38]

$$D_0 = 0.21(kT_0)\ 1.5/(p\ d^2\sqrt{m}) \tag{19}$$

with p is the gas pressure and

$$d = (d_1 + d_2)/2 \tag{20}$$

$$m = \frac{2m_1m_2}{m_1 + m_2} \tag{21}$$

where d_i and m_i are the diameters and masses, respectively, of the particles involved.

The thermal expansion of the gas inside the tube causes an average convection velocity from the center to the ends of the tube:[39]

$$\bar{v}_c = \alpha z/T \tag{22}$$

where α is the heating rate and z is the distance from the center. The average loss of analyte vapor by expulsion becomes

$$f_{lc} = \frac{\alpha}{4T} Y_t(t) \tag{23}$$

Using Equations 16 to 18 and 23, one finds for the total loss rate

$$f_l = \left[\frac{8D_0}{l_a^2}\left(\frac{T}{T_0}\right)^n + \frac{\alpha}{4T}\right] Y_t(t) \tag{24}$$

D. The Degree of Dissociation in the Furnace

Analyte species vaporizing in molecular form can be dissociated in the gas phase of the furnace. Statistical thermodynamics provides the following expression for the dissociation constant K_d:[40]

$$K_d = \frac{n_A n_X}{n_{AX}} = \frac{Z_A(T)\ Z_X(T)}{Z_{AX}(T)} (m_A m_X/m_{AX})^{3/2}$$
$$(2\ \pi\ kT/h^2)^{3/2} \exp(-E_d/kT) \tag{25}$$

n_{AX} is the number density, Z_{AX} the electronic partition function, m_{AX} the mass, and E_d the dissociation energy, respectively, of the molecule. The quantities with the subscripts A and X have the equivalent meanings for the atoms. When a number of molecules, Y_t, is introduced into the atomizer volume then the number of atoms formed by dissociation becomes:

$$Y_A = F\, T^{3/4}\, Y_t^{1/2} \exp(-E_d/2kT) \tag{26}$$

where F is constant and $Y_A \leqslant Y_t$.

E. Numerical Model Calculations

For numerical calculations the following temperature-time functions have been used.

1. Pulse-heated furnace with vaporization from the tube wall:

$$T_w(t) = T_c + \alpha\, t \quad \text{if} \quad 0 \leqslant t < t_{ra} \equiv \frac{T_f - T_c}{\alpha} \tag{27}$$

$$T_w(t) = T_f \qquad \text{if} \quad t \geqslant t_{ra} \tag{28}$$

2. Pulse-heated furnace with vaporization from the platform: $T_w(t)$ corresponding to Equations 27 and 28 but a platform temperature is introduced:

$$T_p(t) = T_w - \Delta\, T_p(t) \tag{28a}$$

The parameters ΔT_{po}, ΔT_{pmax}, and t_{end} were taken from the measurements discussed in Section III.D.

3. Constant temperature furnace:

$$T_w(t) = T_f \quad \text{if} \quad t \geqslant 0 \tag{29}$$

$$\Delta T_p = \Delta T_{po} + \Delta T_{pmax}\, t/t_{ra} \text{ if } 0 \leqslant t < t_{ra} \tag{30}$$

$$\Delta T_p = \Delta T_{po} + \Delta T_{pmax} \frac{t_{end}-t}{t_{end}-t_{ra}} \text{ if } t_{ra} \leqslant t \leqslant t_{end} \tag{31}$$

attributed to the atomizer tube,

$$T_v(t) = T_{vc} + \alpha\, t \text{ if } 0 \leqslant t < t_{vra} \equiv \frac{T_{vf} - T_{vc}}{\alpha_v} \tag{32}$$

$$T_v(t) = T_{vf} \qquad \text{if} \quad t \geqslant t_{vra} \tag{33}$$

is attributed to the vaporizer.

The supply of the analyte is described by the first-order differential Equation 15

$$dX_t/dt = X_t^m\, A \exp(-E_a/kT)$$

where the temperature T corresponds to $T_w(t)$, $T_p(t)$, or $T_v(t)$ for case 1, 2, or 3, respectively.

For the number of analyte atoms in the gas phase we have the following differential equation by using Equations 13 and 24:

$$dY_t/dt = dX_t/dt - \left[\frac{8D_0}{l_a^2}\left(\frac{T}{T_0}\right)^n + \frac{\alpha}{4T}\right] Y_t(t) \tag{34}$$

Here, the temperature T in the brackets means the wall temperature for all cases 1 to 3.

The differential Equations 15 and 34 with the time-dependent temperatures are too complicated to be solved analytically. Therefore, a numerical integration method has been used to develop a computer program for calculating the quantities X_t^r, Y_t^r, Y_a^r, Y_{tint}^r and Y_{aint}^r. The superscript r means that the corresponding quantity without the superscript has been divided by the initial number of analyte atoms introduced into the atomizer.

F. Simplified Calculations of the Atomic Density

Before the results of numerical calculations are discussed, the differential Equations 15 and 34 will be further simplified to get an analytical solution for a rough approximation of the time dependence of the atomic density. In many papers it is assumed that the release rate of the analyte increases linearly with time while a linear temperature increase takes place.[21,24] Assuming a constant release rate appears to be more realistic since X_t in Equation 15 decreases, while the exponential increases. When the release rate is constant and the expression in the bracket of Equation 34 is also constant, one gets

$$\frac{dY_t}{dt} = \frac{N_s}{\tau_v} - \frac{Y_t}{\tau_r} \quad \text{if} \quad 0 \leq t < \tau_v \tag{35}$$

and

$$\frac{dY_t}{dt} - \frac{1}{\tau_r} Y_t = 0 \quad \text{if} \quad t \geq \tau_v \tag{36}$$

The number of analyte atoms within the atomizer volume becomes

$$Y_t(t) = N_s \frac{T_r}{\tau_v} [1 - \exp(-t/\tau_r)] \quad \text{if} \quad 0 \leq t < \tau_v \tag{37}$$

and

$$Y_t(t) = N_s \frac{\tau_r}{\tau_v} [1 - \exp(-\tau_v/\tau_r)] \exp[(\tau_v - t)/\tau_r] \quad \text{if} \quad t \geq \tau_v \tag{38}$$

τ_v means the time necessary to vaporize the analyte amount, N_s, and τ_r is the residence time of the analyte atoms within the atomizer volume. The peak maximum appears at $t = \tau_v$, i.e., when the vaporization is finished. The height of the peak maximum is proportional to the analyte amount introduced and to the ratio of residence time and vaporization time.

The maximum peak height can be achieved if $\tau_v << \tau_r$ where one gets

$$Y_{t,max}(t) = \frac{N_s}{\tau_v} t \quad \text{if} \quad 0 \leqslant t < \tau_v \tag{39}$$

and

$$Y_{t,max}(t) = N_s \exp(-t/\tau_r) \quad \text{if} \quad t \geqslant \tau_v \tag{40}$$

In this case all analyte atoms are within the atomizer volume at the peak maximum.

By using Equations 39 and 40, by integrating the total peak, one finds for the average atomic density:

$$\overline{\eta}_{a,max} = \frac{N_s \tau_r \alpha (T)}{V_a \Delta t} \tag{41}$$

and the efficiency of the atomizer becomes

$$\overline{\eta}_{a,max} = \frac{\tau_r \alpha (T)}{\Delta t} \tag{42}$$

but for the peak maximum

$$\eta_{a,max}^{peak} = \tau_r \alpha (T) \tag{43}$$

The expression in Equation 41 is very similar to that found for the atomizer with continuous sample introduction (see Equation 4).

When the residence time is very short compared to the vaporization time, one finds from Equations 37 and 38:

$$\tau_r \ll \tau_v \quad Y_t(t) \rightarrow N_s \tau_r/\tau_v \quad \text{if} \quad 0 \leqslant t < \tau_v \tag{44}$$

$$Y_t(t) \rightarrow 0 \qquad \text{if} \quad t \geqslant \tau_v \tag{45}$$

The peak of the atomic density shows a plateau of height, $N_s\tau_r/\tau_v$, and the length, τ_v.

Generally, for $\tau_r << \tau_v$ the vaporization rate as a function of time will be observed.

G. Results of Model Calculations

With the computer program based on the model described in Section IV.E, the influence of various parameters on the atomic density within the furnace has been simulated. The results will be shown in the following section.

1. Parameters Influencing the Release Rate

The release rate depends on the activation energy, the frequency factor, and the order of release. As can be seen from Figure 14, an increase of the activation energy causes a higher vaporization temperature but a lower release rate at a given heating rate. The order of release has a similar effect. The influence of the frequency factor on both the vaporization temperature and release is relatively weak.

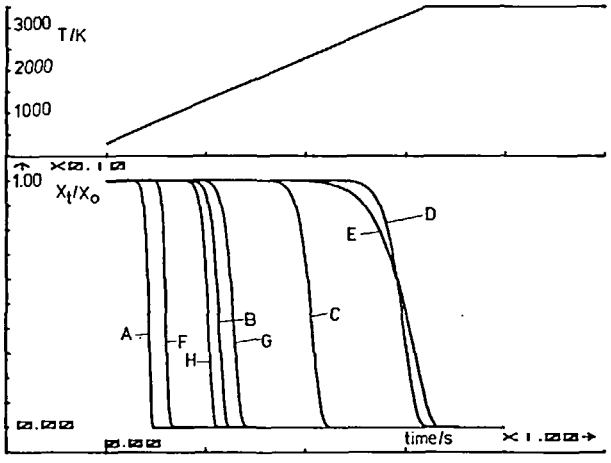

FIGURE 14. Influence of the activation energy, E_a, order of release, m, and frequency factor, A, on the release of adsorbed material. General parameters for A-D; m = 1, A = 1 × $10^{12}s^{-1}$, T_c = 300 K, T_e = 3500 K, α = 1 kK/s^{-1}, l_a = 20 mm, d_a = 6 mm. E_a (kJmol^{-1}) = A, 150; B, 300; C, 500; D, 700. General parameters for E and F: E_a = 300 kJmol^{-1}; A = 1 × 10^{12} s^{-1}. m = E, 0.5; F, 1.5. General parameters for G and H: E_a = 300 kJmol^{-1}, m = 1. A(s^{-1}) = G, 1 × 10^{11}; H, 1 × 10^{13}.

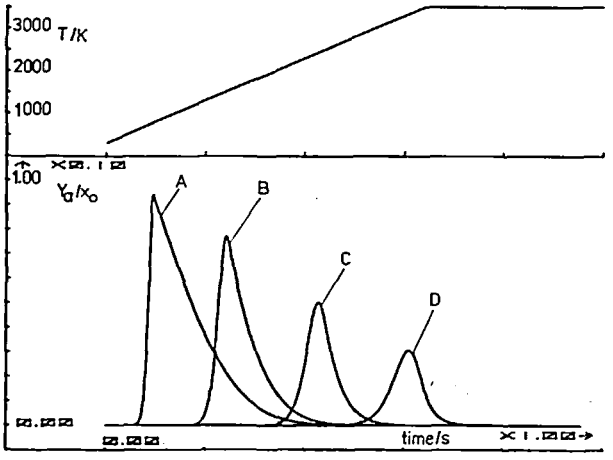

FIGURE 15. Influence of the activation energy, E_a, on the atom population-time dependence in a pulse-heated furnace. General parameters: m = 1, A = 1 × 10^{12} s^{-1}, D_0 = 1 × 10^{-5} m^2 s^{-1}, n = 1.5, l_a = 20 mm, d_a = 6 mm, T_c = 300 K, T_f = 3500 K, α = 1 kK/s. E_a (kJmol^{-1}) = A, 150; B, 300; C, 500; D, 700.

The effect of the activation energy (via the release rate) on the atom population-time dependence in a pulse-heated furnace is shown in Figure 15. The diffusion constant used for this figure corresponds to Ag atoms in Ar. Increasing the activation energy of the analyte release decreases both peak height and peak area.

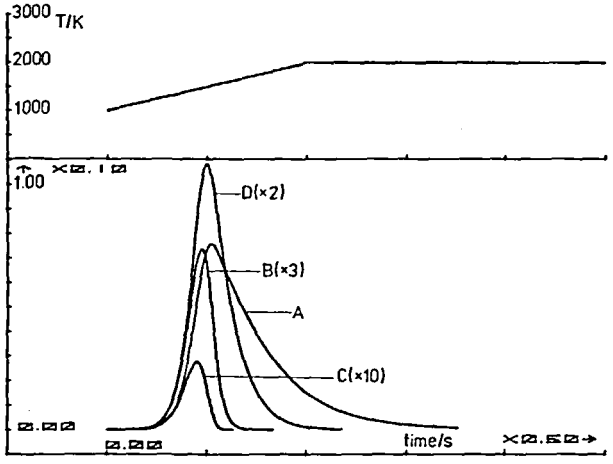

FIGURE 16. Influence of the gas pressure, p, on the atom population-time dependence in a pulse-heated furnace. General parameters: E_a = 300 kJmol^{-1}, A = 1 × 10^{12} s^{-1}, m = 1, n = 1.5, T_c = 1000 K, T_f = 2000 K, α = 1 kK/s, l_a = 20 mm, d_a = 6 mm, gas: Ar, element: Ag. p(hPa) = A, 1000; B, 100; C, 10; D, 1000 (He).

2. Effect of the Diffusion Loss on the Atom Population

Corresponding to Equation 19 there is a linear increase of the diffusion coefficient with the gas pressure. AAS experiments are usually carried out at atmospheric pressure in Ar. But for AES based on the FANES system,[3] the atomization takes place at low gas pressure. The effect of the pressure on the atom population is shown in Figure 16. At a moderate heating rate applied here, the pulses are only slightly shortened by decreasing the pressure but the decrease of the peak height is dramatic. By decreasing the pressure from atmospheric to 10 hPa the atom density is 30-fold lower. Using He instead of Ar causes no severe decrease of the peak's height but the peak area is reduced by a factor of 2.4. At atmospheric pressure (see curve A of Figure 16) the peak height reaches 75% of the ideal atomizer. In other words, a further increase of the gas pressure would not increase the peak height very much. In AAS a rising pressure is accompanied by a decrease of the absorption cross section because of absorption line broadening.[21] The small effect to be expected by a gas pressure above the atmospheric level is further decreased in AAS measurements.

Depending on their masses and atomic diameters the elements have different diffusion coefficients. This effect on the atom population in a pulse-heated furnace is shown in Figure 17, assuming the same activation energy for all elements. As can be seen, there is no remarkable influence of the particular element on the loss rate.

3. Effect of the Temperature Program on the Atom Population

Initial and final temperatures have, at a given ramp rate, only a small influence on the atom population time dependence as can be seen from Figure 18, if the final temperature is at least 200 to 300 K higher than the appearance temperature where the vaporization starts.

The effect of the ramp rate on the atom population is shown in Figure 19. When the ramp rate is higher than 2 kKs^{-1} a further increase will not cause much change in the atom population-time curve. The peak height is increased from 74 to 94% and the peak area decreased by 21%, while the ramp rate varies from 1 to 10 kKs^{-1}. Figure 19 illustrates that the effect of the loss by gas expulsion is relatively weak. At a ramp rate of 2 kKs^{-1} the peak area is changed by 4% and at 4 kKs^{-1} by 6%.

The influence of the ramp rate on the atom population depends on the activation energy

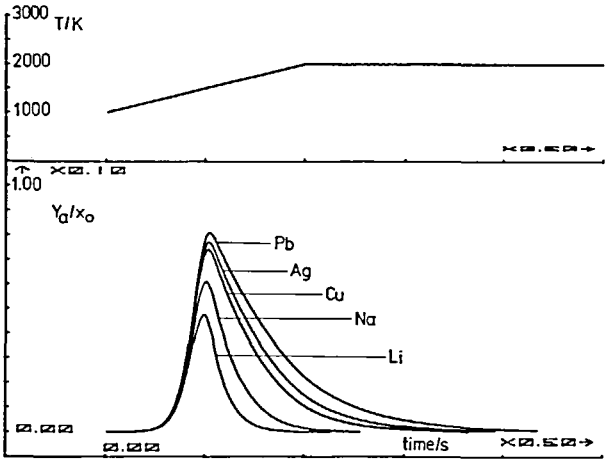

FIGURE 17. Effect of the element evaporated on the atom population-time dependence in a pulse-heated furnace. General parameters: E_a = 300 kJmol^{-1}, A = 1 × 10^{12} s^{-1}, m = 1, n = 1.5, T_c = 1000 K, T_f = 2000 K, α = 1 kK/s, l_a = 20 mm, d_a = 6 mm, gas: Ar, 0.1 MPa.

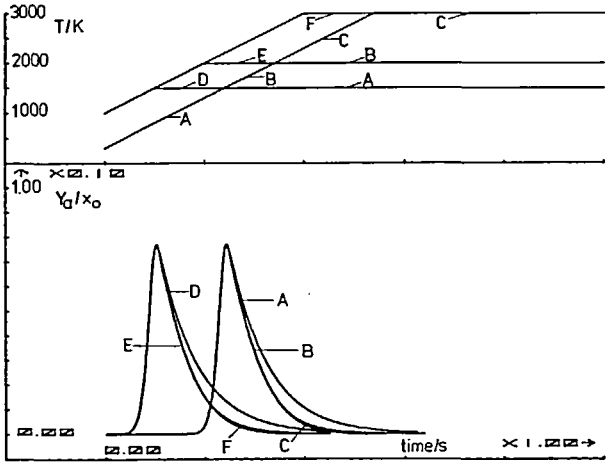

FIGURE 18. Influence of the final temperature on the atom population-time dependence in a pulse-heated furnace. General parameters: E_a = 300 kJmol^{-1}, A = 1 × 10^{12} s^{-1}, m = 1, n = 1.5, D_o = 1 × 10^{-5} m^2 s^{-1}, l_a = 20 mm, d_a = 6 mm, α = 1 kK/s^{-1}. T_c = 300 K for A, B, C; T_f = A, 1500 K; B, 2000 K; C, 3000 K. T_c = 1000 K for D, E, F; T_f = D, 1500 K; E, 2000 K; F, 3000 K.

for the release of the analyte. This is demonstrated in Figure 20. For an element with higher activation energy the effect of the ramp rate on the peak height is also higher. From this point of view the ramp rate applied should be increased for more involatile elements. In practice, electrothermal atomizers provide lower ramp rates at higher temperatures because of the rising radiation losses of the incandescent tube.

4. Influence of Platforms on the Atom Population

In the preceding section it was assumed that the analyte is volatilized in atomic form. If

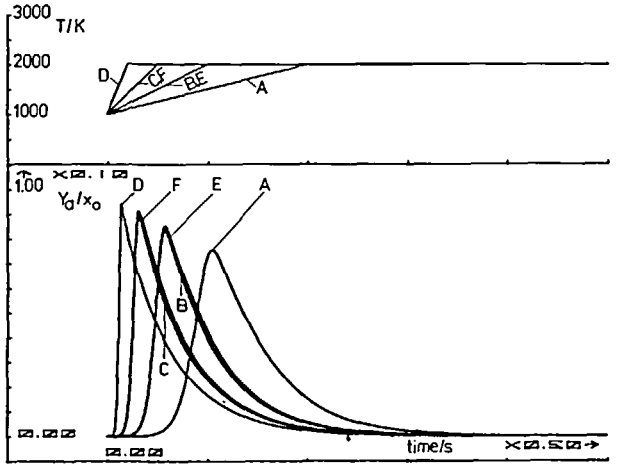

FIGURE 19. Influence of the ramp rate and gas expulsion on the atom population-time dependence in a pulse-heated furnace. General parameters: E_a = 300 kJmol^{-1}, A = 1 × 10^{12} s^{-1}, m = 1, n = 1.5, D_o = 1 × 10^{-5} m^2 s^{-1}, l_a = 20 mm, d_a = 6 mm, T_c = 1000 K, T_f = 2000 K. α (kK/s^{-1}) = A, 1; B, 2; C, 4; D, 10; E, 2 (gas expulsion omitted); F, 4 (gas expulsion omitted).

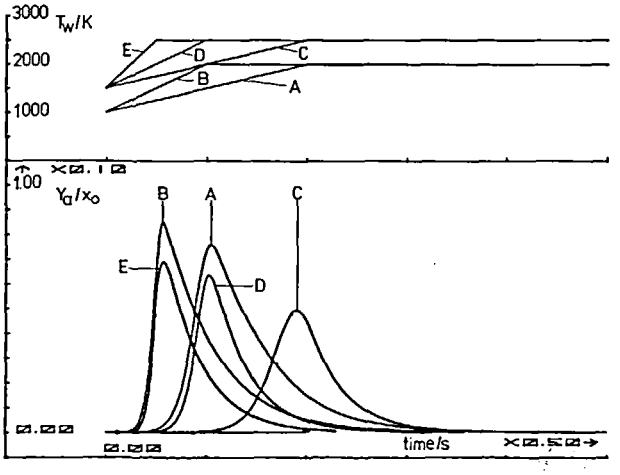

FIGURE 20. Influence of the ramp rate on the atom population-time dependence for analytes with different volatility in a pulse-heated furnace. General parameters: A = 1 × 10^{12} s^{-1}, m = 1, n = 1.5, D_o = 1 × 10^{-5} m^2 s^{-1}, l_a = 20 mm, d_a = 6 mm. For A and B: E_a = 300 kJmol^{-1}, T_c = 1000 K, T_f = 2000 K; α (kK/s^{-1}) = A, 1; B, 2. For C - E: E_a = 500 kJmol^{-1}, T_c = 1500 K, T_f = 2500 K; α (kK/s^{-1}) = C, 1; D, 2; E, 4.

the analyte enters the gas phase as a molecule, then a subsequent step of dissociation has to take place before analyte atoms are observable within the atomizer volume. During volatilization and dissociation of the analyte molecules, a part of them may be lost with the result of a decrease in the relative atom population. Furthermore, it should be noticed that the degree of dissociation is not only a function of the temperature but also of the density of the partners involved in the chemical interaction (see Equations 25 and 26). It is worthwhile

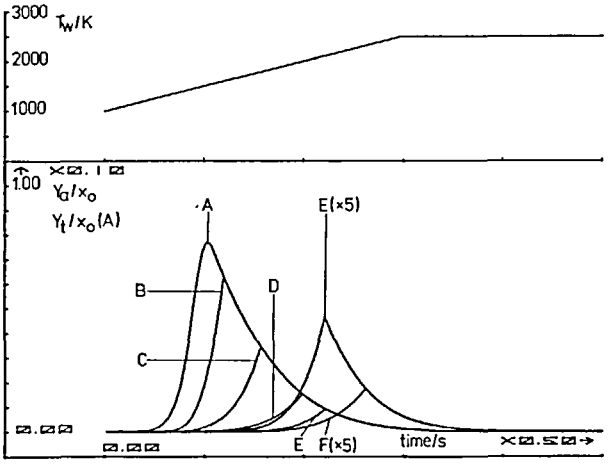

FIGURE 21. Influence of the volatilization of analyte molecules on the atom population-time dependence in a pulse-heated furnace. General parameters: E_a = 300 kJmol^{-1}, A = 1 × 10^{12} s^{-1}, m = 1, n = 1.5, D_o = 1 × 10^{-5} m^2 s^{-1}, l_a = 20 mm, d_a = 6 mm, T_c = 1000 K, T_f = 2500 K, α = 1 kKs^{-1}. A: total relative number of analyte atoms. For B, C: E_d = 500 kJmol^{-1}; m_o (ng Ag) = B, 0.1; C, 10; D, 1000: For D, E: E_d = 700 kJmol^{-1}; m_o (ng Ag) = E, 0.1; F, 10.

to mention here that the chemical equilibria can be considered as being established within the furnace. At atmospheric pressure, gas kinetic collision frequencies are on the order of 10^8 sec^{-1}; consequently, there are many collisions during the time constants involved in the kinetics of GFs.

The effect of the volatilization of analyte molecules can be seen in Figure 21. With higher dissociation energy the atom formation occurs later, causing a decrease of both peak height and peak area. Obviously, the incomplete dissociation of molecules containing the analyte might be avoided by using a very rapid heating.[25] If such a high ramp rate is not available as in most instruments, a platform can be used to delay the volatilization. The effect of the platform can be seen in Figures 22 and 23. As for curve C, the temperature delay by the platform shifts the vaporization into a temperature range of the gas phase where the molecules containing the analyte are dissociated. This can be achieved only partly for a higher dissociation energy (see curve F). The two different platforms used for the calculations cause almost the same effect on the atom population-time curves (see Figures 22 and 23). To dissociate molecules with high dissociation energy more efficiently, platforms which cause a higher temperature difference to that of the tube wall should be used.

The effect of the platform is beneficial both to decrease the matrix interferences and to increase the efficiency of the atomizer. The more complete dissociation of matrix constituents by using the platform causes less chemical interferences and, in AAS experiments, less background absorption.[9,10] This is the purpose of the use of platforms in many cases. But for molecules with high bond energy which contain the analyte, the platform may also increase the sensitivity in AAS compared to determination from the wall. For example, this was observed by Sukhoveeva et al.[41] when they determined Ga chloride samples in a pulse-heated furnace.

5. *Atom Population in Constant Temperature Atomizers*

In the following it is assumed that the atomizer tube has reached its final equilibrium

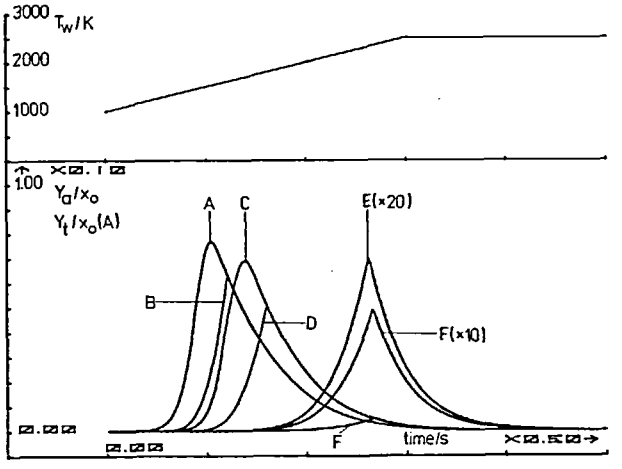

FIGURE 22. Influence of the volatilization of analyte molecules on the atom population-time dependence in a pulse-heated furnace with and without platform (Perkin-Elmer type). General parameters: E_a = 300 kJmol^{-1}, A = 1 × 10^{12} s^{-1}, m = 1, n = 1.5, D_o = 1 × 10^{-5} m^2 s^{-1}, l_a = 20 mm, d_a = 6 mm, T_c = 1000 K, T_f = 2500 K, α = 1 kK/s^{-1}, ΔT_{po} = 30 K, $\Delta T_{p\,max}$ = 350 K, t_{end} = 3 s. For A, B, E, wall volatilization; A, total relative number of analyte atoms; for B - D: E = 500 kJmol^{-1}; m_o (ng Ag) = B (wall), 0.1; C (platform), 0.1; D (platform), 10. For E, F, E_d = 700 kJmol^{-1}, m_o = 10 ng Ag; E, wall; F, platform.

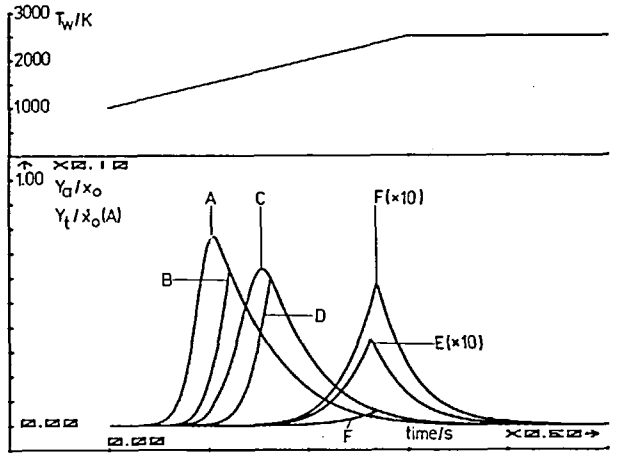

FIGURE 23. Influence of the volatilization of analyte molecules on the atom population-time dependence in a pulse-heated furnace with and without platform (pin type). General parameters: E_a = 300 kJmol^{-1}, A = 1 × 10^{12} s^{-1}, m = 1, n = 1.5, D_o = 1 × 10^{-5} m^2 s^{-1}, l_a = 20 mm, d_a = 6 mm, T_c = 1000 K, T_f = 2500 K, α = 1 kK/s^{-1}, ΔT_{po} = 0, $\Delta T_{p\,max}$ = 550 K, t_{end} = 3 s. For A, B, E, wall volatilization; A, total relative number of analyte atoms; for B - D: E = 500 kJmol^{-1}; m_o (ng Ag) = B (wall), 0.1; C (platform), 0.1; D (platform), 10. For E, F: E_d = 700 kJmol^{-1}, m_o = 10 ng Ag; E, wall; F, platform.

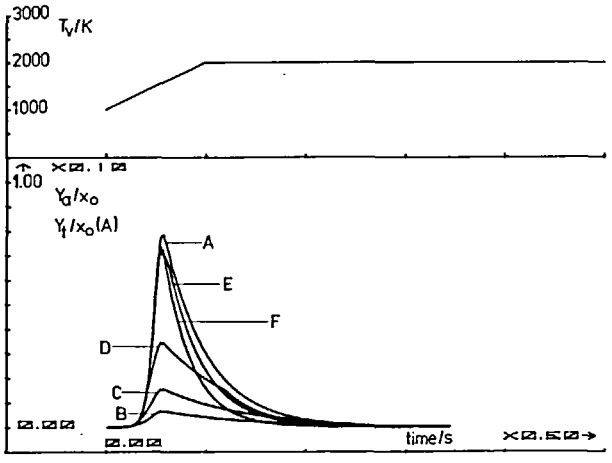

FIGURE 24. Influence of the atomizer temperature on the atom population-time dependence in a constant temperature furnace. General parameters: E_a = 300 kJmol^{-1}, E_d = 700 kJmol^{-1}, A = 1 × 10^{12} s^{-1}, m = 1, n = 1.5, D_o = 1 × 10^{-5} m^2 s^{-1}, l_a = 20 mm, d_a = 6 mm, T_{vc} = 1000 K, T_{vf} = 2000 K, α_v = 2 kK/s^{-1}, m_o = 10 ng Ag. T_w(K) = A (total relative number of analyte atoms), 2200; B, 2200; C, 2300; D, 2400; E, 2500; F, 2900.

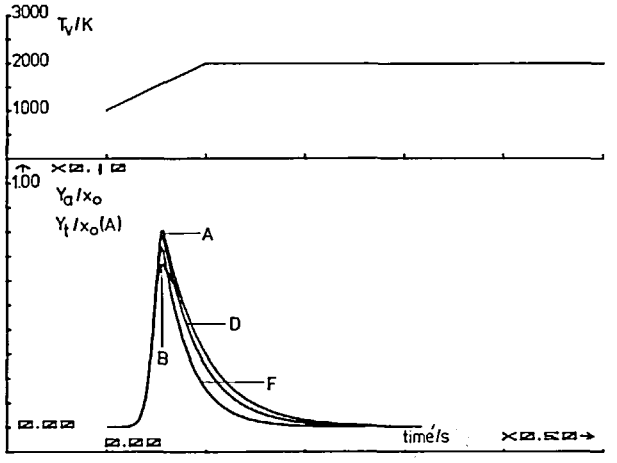

FIGURE 25. Influence of the atomizer temperature on the atom population-time dependence in a constant temperature furnace. General parameters: E_a = 300 kJmol^{-1}, E_d = 700 kJmol^{-1}, A = 1 × 10^{12} s^{-1}, m = 1, n = 1.5, D_o = 1 × 10^{-5} m^2 s^{-1}, l_a = 20 mm, d_a = 6 mm, t_{vc} = 1000 K, T_{vf} = 2000 K, α_v = 2 kK/s^{-1}, m_o = 0.1 ng Ag, T_w(K) = A (total relative number of analyte atoms), 2200; B, 2200; D, 2400; F, 2900.

temperature before the vaporizer starts to be heated separately. The volume of the vaporizer is assumed to be negligible compared to that of the atomizer.

Figure 24 shows the increase of the atom population with the temperature of the atomizer. At 2500 K the dissociation is practically complete. A higher temperature leads to an increase of the diffusion losses. The atomization efficiency can be as high as 72% at the peak maximum. As can be seen from Figure 25, a complete dissociation of the molecules con-

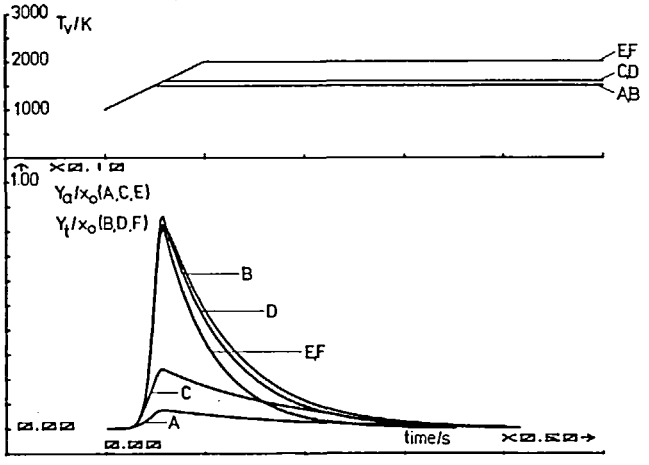

FIGURE 26. Influence of the temperature regime on the population-time dependence of atoms and molecules in a constant temperature furnace. General parameters: E_a = 300 kJmol^{-1}, E_d = 500 kJmol^{-1}, A = 1 × 10^{12} s^{-1}, m = 1, n = 1.5, D_o = 1 × 10^{-5} m^2 s^{-1}, l_a = 20 mm, d_a = 6 mm, T_{vc} = 1000 K, α_v = 2 kK/s^{-1}, m_o = 10 ng Ag. Relative number of atoms: A, C, E; relative total number: B, D, F. A, B: T_{vf} = 1500 K, T_w = 1600 K; C, D: T_{vf} = 1600 K, T_w = 1700 K; E, F: T_{vf} = 2000 K, T_w = 2000 K.

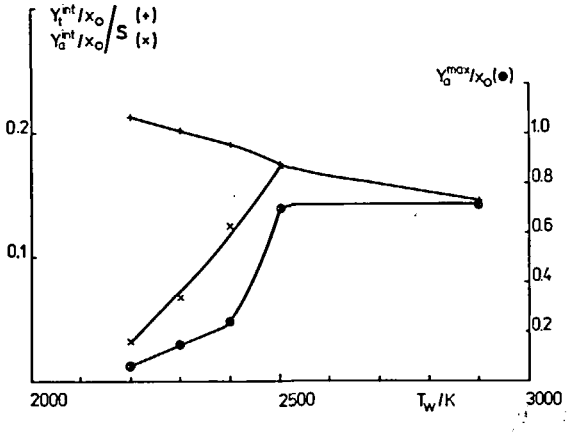

FIGURE 27. Influence of the atomizer temperature on the integrated and maximum relative numbers of analyte atoms in a constant temperature furnace. +, total number; x, ⊗, number dissociated.

taining the analyte will be reached at a lower temperature if a lower analyte concentration is present.

The optimization of the temperature regime is shown in Figure 26. As a result, an efficiency of 81% can be reached at the peak maximum. The integrated and peak values of the relative numbers of the analyte atoms for the constant temperature furnace as a function of the atomizer temperature are shown in Figure 27. After a steep rise within several hundred degrees Kelvin, the population density remains nearly constant. The decrease after the maximum is more pronounced for the integrated signal because of the influence of the losses on the tail of the density curve.

6. Comparison of Calculated Atom Populations with Efficiency Measurements

Sturgeon and Berman[14] published a study on the efficiency of GFs for AAS continuing the work of Van den Broek and deGalan.[42] They determined the efficiency of a pulse-heated commercial furnace (HGA-2200) for several elements. The atom population within the atomizer has been determined by measuring electron densities that are correlated to ion densities of the analyte as well as by measuring the atomic absorption. They found atomizer efficiencies corresponding to the peak maximum ranging from 1 to 30%.

Frech et al.[9] published a comparison of the characteristic masses for peakheight AA measurements (pg/0.0044 A) using various pulse-heated furnaces and their own constant temperature furnace at optimum conditions. When normalized to a 1-mm²-tube area these sensitivities agreed for the pulse-heated furnaces for the elements investigated within a factor of two. For the elements Ag, Cd, Mn, and Pb the experimental sensitivities, in particular those for the constant temperature furnace, were close to the attainable maximum. The efficiencies for the pulse-heated furnace are about 50% for these elements. An exception was Al where the efficiency was only 10%. Frech et al.[9] reported on a further increase in sensitivity by using caps to reduce the cross section at the tube ends and a plug in the injection port. For Pb the improvement in the peak height was only 22% by these measures, whereas the peak area increased by 86%. About half of the gain in the peak height can be attributed to the effect of the plug. In agreement with other experiments, the results with the constant temperature furnace have shown that the loss rate of atomic vapor through the injection port is relatively small, not exceeding 20% of the total loss rate.[21]

For elements with low boiling temperatures, such as the alkaline elements and Zn, Mg, Cd, and Ag, the condition $\tau_v << \tau_r$ is met, i.e., the vaporization is sufficiently fast in experiments with the usual commercial instruments. The results of Sturgeon and Berman[14] have shown that there is an inverse correlation between the efficiency of the furnace and the vaporization time. The question arises whether the low efficiencies for several elements are a result of a too-small heating rate of the furnace at the vaporization temperature of these elements or whether their release mechanism is different. For illustration, pulse characteristics measured by Sturgeon and Berman[14] together with the heating characteristics are shown in Table 2. As can be seen from Table 2 there is a drastic drop of the heating rate of the furnace at temperatures above 2500 K.

The model described in the preceding sections will be applied to elements from Table 2. To adapt the model to the real experimental conditions, which are characterized by a strongly decreasing ramp rate at higher temperatures, the ramp rate was assumed to consist of two parts with different slopes approximating the heating curve within the temperature interval of the vaporization.

Figure 28 shows the model calculations for Al. The appearance and peak maximum temperatures and the efficiency calculated agree satisfactorily with the values measured, when the ramp rates applied in the experiments are used (see Figure 28B). The efficiency is expected to be about 50% for optimum heating conditions (see Figure 28C,D). In the case of Al it is not necessary that the formation of AlO must be assumed to explain the low efficiency of atomization observed for that element.[14]

For the volatile element Cs, atom population-time curves are shown in Figure 29. Here, the temperature program used in the experiment was already near the optimum. Appearance and peak maximum temperatures agree satisfactorily with the experiments, the efficiency is too large by a factor of two (see Table 2). This latter deviation corresponds to the uncertainly of the efficiency values.[14]

The experimental pulse characteristics for Ba cannot be met by model curves when a first-order release process (m = 1) is assumed. This is evident from Figure 30, where the appearance temperature calculated agrees with the experimental value but the pulses are too sharp and the efficiency is 50 to 70%. To get broader peaks, the model needs to assume a

Table 2
ATOMIZER EFFICIENCIES $\bar{\eta}_a$, ABSORBANCE PULSE CHARACTERISTICS, HEATING RATES DURING VAPORATION α_v, AND ACTIVATION ENERGIES E_a CORRESPONDING TO THE APPEARANCE TEMPERATURES FOR SEVERAL ELEMENTS[14] AND COMPARISON WITH MODEL CALCULATIONS

Element	T_{appear} (K)	T_{peak} (K)	τ_v (ms)	$\bar{\eta}_{ap}$ (%)	α_v (K/s)	E_a kJmol^{-1}	m	Model calculations
Al	2180	2480	370	9	650—400	550	(1)	Figure 28B
	(2160)[a]	(2520)		(12)		(550)		
K	1410	1880	425	19	1500—1000	360		
Rb	1410	1910	450	20	1500—970	360		
Cs	1460	1990	500	30	1500—800	370	(1)	Figure 29B
	(1500)	(1840)		(60)		(370)		
Na	1240	1800	500	15	1500—1200	310		
Ca	1850	2550	900	6	1150—350	470		
Ba	1720	2480	1020	6	1500—400	410	(0.5)	Figure 30C
	(1800)	(2570)		(11)		(250)		
Ga	1420	2560	1430	4	1500—350	360		
Sr	1820	2710	1430	1	1200—220	460	(0.5)	
	(1850)	(2620)		(6)		(250)		

Results of model calculations are given in parenthesis.

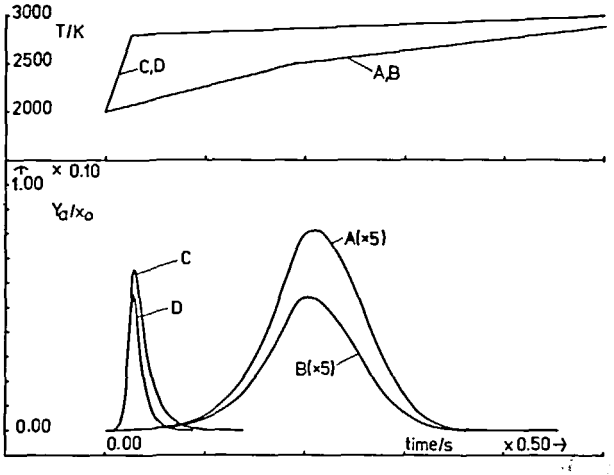

FIGURE 28. Model calculations of the Al atom population-time dependence in a pulse-heated furnace with various heating characteristics. General parameters: E_a = 550 kJmol^{-1}, A = 1 × 10^{12} s^{-1}, m = 1, D_o = 1.89 × 10^{-5} m^2 s^{-1}, l_a = 20 mm, d_a = 6 mm, T_c = 2000 K, m_o = 2 ng. For A, B: T_{f1} = 2500 K, α_1 = 525 Ks^{-1}, T_{f2} = 3000 K, α_2 = 250 Ks^{-1}. For C, D: T_{f1} = 2800 K, α_1 = 6 kKs^{-1}, T_{f2} = 3000 K, α_2 = 250 Ks^{-};1. For A, C: n = 1.5; for B, D: n = 1.7.

slower release mechanism. This has been done to calculate curve C in Figure 30. Here, assuming m = 0.5 and E_a = 250 kJmol^{-1}, pulse characteristics as well as efficiency agree more satisfactorily with the experimental finding.

A similar situation is found for Sr, as can be seen from Figure 31. The small efficiency and broad pulses measured in this case cannot be explained within the model by a too-low heating rate of the furnace as for Al but by assuming a slower release process. An increase

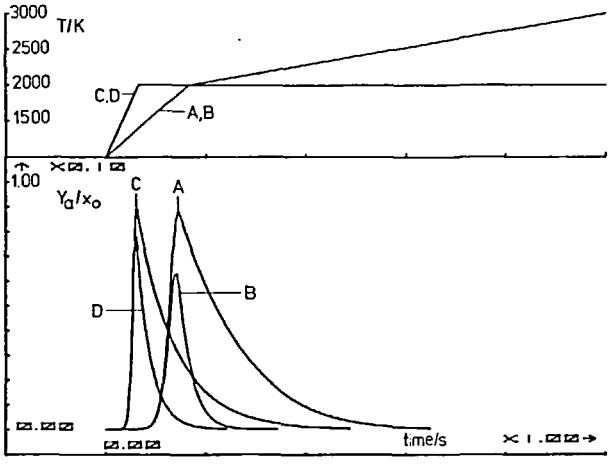

FIGURE 29. Model calculations of the Cs atom population-time dependence in a pulse-heated furnace with various heating rates. General parameters: E_a = 370 kJmol^{-1}, A = 1 × 10^{12} s^{-};1, m = 1, D_o = 6.39 × 10^{-6} m^2 s^{-1}, d_a = 6 mm, T_c = 1000 K, m_o = 0.5 ng. For A, B: T_{f1} = 2000 K, α_1 = 1.2 kKs^{-1}, T_{f2} = 3000 K, α_2 = 0.25 kKs^{-1}. For C, D: T_{f1} = 2000 K, α_1 = 3 kKs^{-1}, T_{f2} = 2000 K, α_2 = 0. For A, C: l_a = 27 mm, n = 1.5. For B, D: l_a = 20 mm, n = 2.

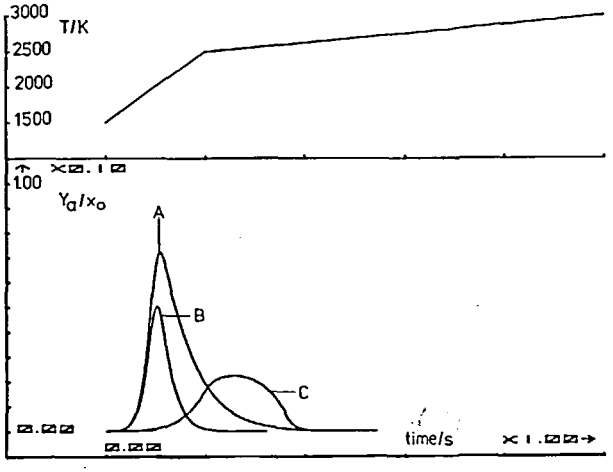

FIGURE 30. Model calculations of the Ba atom population-time dependence in a pulse-heated furnace. General parameters: A = 1 × 10^{12} s^{-1}, D_o = 6.07 × 10^{-6} m^2 s^{-1}, l_a = 20 mm, d_a = 6 mm, T_c = 1500 K, T_{f1} = 2500 K, α_1 = 1 kKs^{-1}, T_{f2} = 3000 K, α_2 = 0.25 kKs^{-1}, m_o = 5 ng. For A, B: E_a = 410 kJmol^{-1}, m = 1, n = A, 1.5; B, 2. For C: E_a = 250 kJmol^{-1}, m = 0.5, n = 2.

of the heating rate as high as 3 kKs^{-1} is not sufficient for an efficiency near 50% (see Figure 31D).

Whether the values for m and E_a used in the case of Ba and Sr have any real physical meaning is not yet clear. At least that combination of m and E_a slows down the release rate of the analyte to the extent necessary.

In context with the model calculations, more experimental findings should be considered.

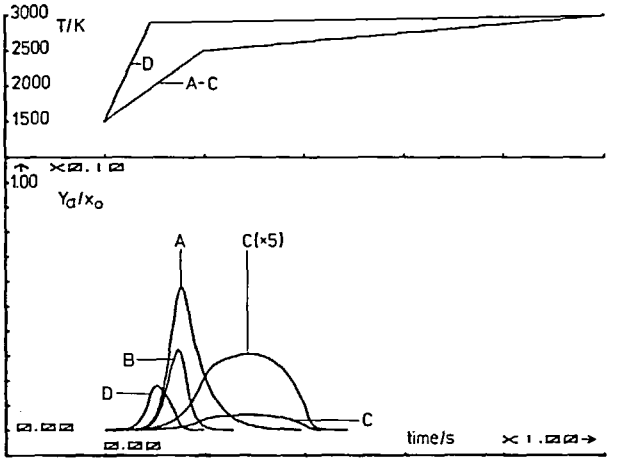

FIGURE 31. Model calculations of the Sr atom population-time dependence in a pulse-heated furnace. General parameters: A = 1 × 10^{12} s^{-1}, D_o = 9.04 × 10^{-6} m^2 s^{-1}, l_a = 20 mm, d_a = 6 mm, T_c = 1500 K, T_{f2} = 3000 K, α_2 = 0.25 kKs^{-1}, m_o = 1 ng. For A, B, C: T_{f1} = 2500 K, α_1 = 1 kKs^{-1}. For D: T_{f2} = 2900 K, α_1 = 3 kKs^{-1}. For A, B: E_a = 460 $kJmol^{-1}$, m = 1. n = A, 1.5; B, 2; C, 2; D, 2. For D, C: E_a = 270 $kJmol^{-1}$, m = 0.5.

The experiments of Chakrabarti et al.[43] using the capacitive discharge technique of pulse heating reaching heating rates of 40 − 75 kKs^{-1} have shown that for many elements considerable sensitivity enhancements may be achieved. These enhancements range from 3- to 5.6-fold for Pb, Cu, Zn, Cd, Al, Ni, Mn, and Mg when the fast-heated furnace is compared with the usual system. This means that for many elements the efficiency comes close to the theoretical maximum.

The increase in sensitivity for elements such as Ba, Ga, and Sr to efficiencies higher than 20% by using tantalum or tungsten surfaces for atomization shows the limitations of graphite surfaces in this case.[44,45]

7. Conclusions from the Model Calculations

The preceding sections have shown that the understanding of the basic processes going on in GFs is sufficient for the formation of an adequate mathematical model. With the help of that model, the evaluation of the optimum conditions for the design and operation of a furnace for its intended purpose may be realized. This refers in particular to the dimensions and the heating program to be used for solving a given analytical problem. The most severe uncertainty in the description of the model comes from the interaction processes between sample and atomizer surface. But the chemical characterization of graphite materials has been improved during the last few years, and this has been reviewed by Holcombe and Koirtyohann.[46]

A comprehensive study of the thermodynamic equilibria of species in the gas phase of GFs with respect to reduced interference effects has recently been published by Frech et al.[47] This review provides data on the chemical reactions that are necessary to carry out model calculations.

Using an adequate model for the GF atomizer incorporated into a computer program, it should be possible to reduce considerably the experimental effort to find the optimum conditions or a given analytical task.

The description of the GF given in this review is not limited to AAS — it can be used

in AES and LAFS, too.[3,48] In particular, for GFAES and FANES, the model is useful when the need for a separate control of volatilization/atomization and excitation has to be fulfilled. Furthermore, the considerable analytical experience from GFAAS may be transferred to the developing fields of GF AES and multielement AAS.

APPENDIX

Symbols Glossary

A	—	(preexponential) frequency factor of the release function, s
C_{st}	—	heat capacity of the tube atomizer, WsK^{-1}
D_o	—	diffusion constant, m^2s^{-1}
d_a	—	atomizer diameter, m
E_a	—	activation energy of release, $kJmol^{-1}$
E_d	—	dissociation energy, $kJmol^{-1}$
H_o	—	sticking probability, ≤ 1
l_a	—	atomizer length, m
m	—	order of release, $0 \leq m \leq 1$
m_a	—	atomic mass unit, 1.66 E-27 kg
m_o	—	initial mass of the analyte, kg
M	—	relative atomic mass
n	—	gas combination factor, $1.5 \leq n \leq 2$
n_a	—	atomic density, m^{-3}
N_s	—	number of sample atoms
$\dot{N}_s$	—	sample introduction rate, s^{-1}
p	—	pressure, Pa
P_a	—	electric power applied to the atomizer tube, W
P_l	—	overall heat loss of the tube atomizer, W
R	—	gas constant, 8.314 E-3 kJ $K^{-1}mol^{-1}$
T	—	thermodynamic temperature, K
T_x	—	various temperatures, K, where x means: ap — appearance; c — charring or pyrolysis; f — final; g — gas; p — platform; s — surface; v — vaporization; w — wall
t	—	time, s
v_c	—	convection velocity inside atomizer volume, ms^{-1}
V_a	—	atomizer volume, m^3
α	—	ramp rate at the center of the atomizer ($\equiv d T_w/dt$), Ks^{-1}
$\alpha(T)$	—	degree of dissociation, $\alpha(T) \leq 1$
γ	—	parameter quantifying the deviation of a tube atomizer from isothermal conditions
η_a	—	atomizer efficiency, $0 \leq \eta_a \leq 1$
t_e, t_r	—	evaporation and residence time, respectively, s

REFERENCES

1. **Falk, H.,** Analytical capabilities of atomic spectrometric methods using tunable lasers: a theoretical approach, *Prog. Anal. Atom. Spectrosc.*, 3, 181, 1980.
2. **Alkemade, C. T. J.,** Atomic physics and atomic spectroscopy: mother and daughter?, *Spectrochim. Acta*, 38B, 1395, 1983.

3. **Falk, H., Hoffmann, E., and Luedke, C.,** A comparison of furnace atomic nonthermal excitation spectrometry (FANES) with other atomic spectroscopic techniques, *Spectrochim. Acta,* 39B, 283, 1984.
4. **Kantor, T.,** New approaches to the separation of evaporation and atomization — excitation in atomic spectrometry, *Spectrochim. Acta,* 38B, 1483, 1983.
5. **Johnson, D. J., Sharp, B. L., West, T. S., and Dagnall, R. M.,** Some observations on the vaporation and atomization of samples with a carbon filament atomizer, *Anal. Chem.,* 47, 1234, 1975.
6. **Nakahara, T.,** Application of hydride generation techniques in atomic absorption, atomic fluorescence and plasma atomic emission spectroscopy, *Prog. Anal. Atom. Spectrosc.,* 6, 163, 1983.
7. **Chakrabarti, C. L., Shaole, Wu., Karwowska, R., Rogers, J. T., and Dick, R.,** The gas temperature in and the gas expulsion from a graphite furnace used for AAS, *Spectrochim. Acta,* 40B, 1663, 1985.
8. **Slavin, W. and Manning, D. C.,** The graphite probe constant temperature furnace, *Spectrochim. Acta,* 37B, 955, 1982.
9. **Frech, W., Cedergren, A., Lundberg, E., and Siemer, D. D.,** Electrothermal AAS: present understanding and future needs, *Spectrochim. Acta,* 38B, 1435, 1983.
10. **Slavin, W., Carnrick, G. R., Manning, D. C., and Pruszkowska, E.,** Recent experience with stabilized temperature platform furnace and Zeeman background correction, *At. Spectrosc.,* 4, 69, 1983.
11. **Holcombe, J. A. and Sheehan, M. T.,** Graphite furnace modification for second surface atomization, *Appl. Spectrosc.,* 36, 631, 1982.
12. **Slavin, W., Manning, D. C., and Carnrick, G. R.,** The stabilized temperature platform furnace, *At. Spectrosc.,* 2, 137, 1981.
13. **Harnly, J. M. and Beecher, G. R.,** Signal to noise ratios for flow injection atomic absorption spectrometry, *J. Anal. Atom. Spectrom.,* 1, 75, 1986.
14. **Sturgeon, R. E. and Berman, S. S.,** Determination of the efficiency of the graphite furnace for atomic absorption spectrometry, *Anal. Chem.,* 55, 190, 1983.
15. **Slavin, W.,** *Graphite Furnace AAS: a Source Book,* Perkin-Elmer Corp., Norwalk, Conn., 1984.
16. **Marshall, J., Littlejohn, D., Ottaway, J. M., Harnly, J. M., Müller-Ihli, N. J., and O'Haver, T. C.,** Simultaneous multi-element analysis by carbon furnace atomic-emission spectrometry, *Analyst,* 108, 178, 1983.
17. **Bolshov, M. A., Zybin, A. V., Koloshnikov, V. G., Mayorov, I. A., and Smirenkina, I. I.,** Laser-excited fluorescence analysis with electrothermal sample atomization in vacuum, *Spectrochim. Acta,* 41B, 487, 1986.
18. **Tilch, J., Falk, H., Paetzold, H.-J., Mon, P. G., and Schmidt, K. P.,** Application of the laser-excited atomic fluorescence on the determination of trace elements in solids, *Coll. Spectrosc. Int. XXIV,* TUG 067, 1985.
19. **Matusiewicz, H. and Barnes, R. M.,** Determination of Al and Si in biological materials by ICP AES with electrothermal vaporization, *Spectrochim. Acta,* 39B, 891, 1984.
20. **Long, S. E. and Snook, R. D.,** Some observations on electrothermal vaporization for sample introduction into ICP, *Spectrochim. Acta,* 40B, 553, 1985.
21. **Sturgeon, R. E. and Chakrabarti, C. L.,** Recent advances in electrothermal atomization in graphite furnace atomic absorption spectrometry, *Prog. Anal. Atom. Spectrosc.,* 1, 5, 1978.
22. **Lawson, S. R., Dewalt, F. G., and Woodriff, R.,** Influence of furnace design on operation, sensitivity and matrix interferences in electrothermal atomic absorption spectrometry, *Prog. Anal. Atom. Spectrosc.,* 6, 1, 1983.
23. **Massmann, H.,** The comparison of AA and AF in the graphite cuvette, *Spectrochim. Acta,* 23B, 215, 1968.
24. **L'vov, B. V.,** Electrothermal atomization — the way toward absolute methods of AAS, *Spectrochim. Acta,* 33B, 153, 1978.
25. **Chang, S. B. and Chakrabarti, C. L.,** Factors affecting atomization in graphite furnace atomic absorption spectrometry, *Prog. Anal. Atom. Spectrosc.,* 8, 83, 1985.
26. **L'vov, B. V.,** The analytical use of AA spectra, *Spectrochim. Acta,* 17, 761, 1961.
27. **Falk, H. and Glismann, A.,** Spatially and temporally resolved temperature profiles in graphite furnaces, *Fresenius Z. Anal. Chem.,* 323, 748, 1986.
28. **Gilmutdinov, A. K. and Fishman, I. S.,** The theory of sample transfer in semi-enclosed atomizers for AAS, *Spectrochim. Acta,* 39B, 171, 1984.
29. **Slavin, W., Myers, S. A., and Manning, D. C.,** Reduction of temperature variation in the AA graphite furnace, *Anal. Chim. Acta,* 117, 267, 1980.
30. **Falk, H., Glismann, A., Bergann, L., Minkwitz, G., Schubert, M., and Skole, J.,** Time-dependent temperature distribution of graphite-tube atomizers, *Spectrochim. Acta,* 40B, 533, 1985.
31. **Manning, D. C. and Slavin, W.,** Factors influencing the atomization of vanadium in graphite furnace AAS, *Spectrochim. Acta,* 40B, 461, 1985.
32. **Rademeyer, C. J. and Human, H. G. C.,** Wall and gas temperature distribution in a graphite furnace atomizer, *Prog. Anal. Spectrosc.,* 9, 167, 1986.

33. **Holcombe, J. A. and Rayson, G. D.,** Analyte distribution and reactions within a graphite furnace atomizer, *Prog. Anal. Atom. Spectrosc.*, 6, 225, 1983.
34. **Edelmann, Ch. and Schneider, H. G., Eds.,** *Vakuumphysik und -Technik*, Akadem. Verlagsgesellsch, Geest & Portig K. G., Leipzig, 1978, 71.
35. **Arthur, J. R. and Cho, A. Y.,** Adsorption and desorption kinetics of Cu and Au on (0001) graphite, *Surf. Sci.*, 36, 641, 1973.
36. **Wutz, M., Adam, H., and Walcher, W.,** *Theorie und Praxis der Vakuumtechnik*, Friedrich Vieweg & Sohn, Braunschweig/Wiesbaden, 1982, 36.
37. **L'vov, B. V.,** *Atomic Absorption Spectrochemical Analysis*, Adam Hilger, London, 1970, 287.
38. **Ebert, H., Ed.,** *Physikalisches Taschenbuch*, Friedr. Vieweg & Sohn, Braunschweig, 1967, 220.
39. **Holcombe, J. A.,** Vapor expulsion and loss from a graphite furnace atomizer, *Spectrochim. Acta*, 38B, 609, 1983.
40. **Magyar, B.,** *Guide-Lines to Planning Atomic Spectrometric Analysis*, Akadémiai Kiado, Budapest, 1982, chap. 5.
41. **Sukhoveeva, L. N., Butrimenko, G. G., and Spivakov, B. Ya.,** AA determination of Ga and In in a graphite furnace by vaporization from a substrate, *J. Anal. Chem.*, 55, 1064, 1980.
42. **Van den Broek, W. M. G. T. and de Galan, L.,** Supply and removal of sample vapor in graphite thermal atomizers, *Anal. Chem.*, 49, 2176, 1977.
43. **Chakrabarti, C. L., Hamed, H. A., Wan, C. C., Li, W. C., Bertels, P. C., Gregoire, D. C., and Lee, S.,** Capacitive discharge heating in graphite furnace AAS, *Anal. Chem.*, 52, 167, 1980.
44. **L'vov, B. V. and Pelieva, L. A.,** The efficiency of lining a graphite furnace with Ta foil in AAS, *Can. J. Spectrosc.*, 23, 14, 1978.
45. **Sychra, V., Kolikova, D., Vyskockova, O., and Hlavac, R.,** Electrothermal atomization from metallic surfaces. I. Design and performance of a tungsten-tube atomizer, *Anal. Chim. Acta*, 105, 263, 1979.
46. **Holcombe, J. A. and Koirtyohann, S. R.,** The Downingtown furnace atomic absorption workshop: a report, *Spectrochim. Acta*, 39B, 243, 1984.
47. **Frech, W., Lundberg, E., and Cedergren, A.,** Investigations of some methods used to reduce interference effects in graphite furnace AAS, *Prog. Anal. Atom. Spectrosc.*, 8, 257, 1985.
48. **Marshall, J., Carroll, J., Littlejohn, D., Ottaway, J. M., O'Haver, T. C., and Harnly, J. M.,** Microcomputer controlled background correction for ETA-AES and ETA-continuum source AAS, *Anal. Proc.*, 22, 67, 1985.